AIMS Mathematics, 10(11): 27247–27276.
DOI: 10.3934/math.20251198
Received: 28 September 2025
Revised: 03 November 2025
Accepted: 10 November 2025
Published: 24 November 2025

https://www.aimspress.com/journal/Math

Research article

Solitary waves in elastic materials based on modified strain gradient elasticity

A. R. El-Dhaba*

Department of Mathematics and Statistics, College of Science, King Faisal University, P.O. Box 400, Al-Ahsa 31982, Saudi Arabia

* **Correspondence:** Email: aemam@kfu.edu.sa.

Abstract: In the present study, we derive a Boussinesq–type nonlinear partial differential equation to describe solitary wave propagation in isotropic elastic materials. The mathematical formulation is based on the modified strain gradient elasticity (MSGE) framework, which accounts for micro–deformations arising from micro–structural effects as well as macro–scale deformation due to surface effects. The derivation is based on Hamilton's principle, which equates the variation of the strain energy functional to the virtual work done by external forces. The resulting mathematical model is formulated in tensor form to maintain generality and is subsequently specialized to the one–dimensional case to elucidate the nonlinear nature of solitary wave propagation and the influence of micro–structural effects on the material's dynamic response. A key result of this study is the demonstration that the type of wave propagation in the medium can be controlled by appropriately selecting the length–scale parameter associated with micro–inertia, as well as the material length–scale parameters. Three types of initial and boundary conditions are considered: (i) Constant initial and boundary conditions, (ii) dynamic boundary conditions, and (iii) static initial conditions, moreover; all physical quantities are plotted and discussed in detail.

Keywords: solitary waves; elastic material; MSGE theory; NPDEs; Hamilton's principle; Boussinesq type equation
Mathematics Subject Classification: 74B20, 74J30, 74J35

1. Introduction

Continuum mechanics in its classical form offers a well–established theoretical framework for modeling the static and dynamic responses of elastic materials due to the application of external forces at the macroscopic level. However, this theory is not always accurate in modeling the behavior of materials at the microscopic level. The limitations of this theory are evident in

materials that demonstrate complex behaviors, such as polymers, nanocomposites, metamaterials, bone tissue, and polycrystalline metals, where the interplay between the micro– and macro scales is important for understanding their overall behavior. To overcome these challenges, researchers and scientists introduced have generalized continuum theories, such as strain gradient elasticity, couple stress theory [1], micromorphic models [2], nonlocal continuum theories [3], and microstructure elasticity [4], which have the ability to bridge the gap between continuum mechanics and the underlying microstructural behavior of materials. In contrast to classical continuum mechanics, the generalized continuum theories incorporate additional kinematical variables and material length–scale parameters that allow for more accurate descriptions of microscale phenomena. These generalized frameworks enable the modeling of phenomena including, but not limited to, dispersion in wave propagation, size effects in elastic/plastic materials, and enhanced stiffness in nanostructured materials.

One of these phenomena is wave propagation, which can be studied within both classical and generalized continuum mechanics to provide a robust understanding of how mechanical waves propagate at different scales. In classical continuum mechanics, wave propagation is typically analyzed using linear elasticity, where the material is assumed to be homogeneous and isotropic. This framework allows for the derivation of fundamental wave equations, such as the wave equation and the dispersion relation, which describe wave propagation through elastic materials. However, this approach is not accurate in representing wave propagation in elastic materials that exhibit microstructural effects or nonlocal interactions, which are often observed in advanced materials and biological tissues. On the other hand, generalized continuum mechanics extends the classical theory by incorporating additional parameters that account for microstructural influences, such as the Cosserat [5] and micropolar theories [6–8]. These theories introduce additional degrees of freedom, which can significantly affect waves behavior. For instance, in materials with complex internal structures, the waves speed and attenuation can vary dramatically, depending on the material's microstructure and loading conditions.

One of the important topics in wave propagation that can be modeled by generalized continuum mechanics is solitary wave propagation in elastic materials. These waves have characteristic properties that arise from the interaction between nonlinearity and dispersion within elastic media. Many studies have focused on solitary waves in elastic materials. For instance, Maugin [9] presented a historical review covering the period 1938–2010 on the propagation of soliton waves in elastic materials [10–12].

Numerous studies have focused on the propagation of solitons in elastic materials. However, experimental studies by Fleck et al. [13] and Lam et al. [14] have demonstrated that, at smaller length scales, materials exhibit size–dependent behavior that classical theories cannot capture. This limitation arises because classical models neglect the role of a material's internal structure. The modified strain gradient elasticity theory addresses this issue by incorporating higher–order spatial derivatives of strain into the strain energy density functional. This modification introduces intrinsic material length–scale parameters, allowing the theory to account for size–dependent effects, which are especially significant at the micro- and nanoscales. This theory has found important applications in small–scale engineering systems, such as microelectromechanical systems (MEMS) and nanoelectromechanical systems (NEMS), leading to improved accuracy in modeling and design. Additionally, it enhances the modeling of advanced composite materials, thin films, and biological tissues, where the internal structure plays a critical role in the overall mechanical response [15, 16].

Solitons can also exist in birefringent optical fibers [17], allowing the study of light interactions with the unique properties of these materials. In such fibers, the core is engineered to have different

refractive indices along two orthogonal axes, commonly referred to as the fast and slow axes. This anisotropy causes the polarization state of light to evolve as it propagates through the fiber, leading to phenomena such as polarization mode dispersion (PMD) and polarization–dependent loss. These effects can be either advantageous or challenging, depending on the intended application. Many applications of soliton–enhanced birefringent fibers can be found in telecommunications, sensing, and laser systems.

The study of solitary waves in elastic materials has become a vital area of research due to its significant applications in advanced engineering and metamaterial design, where the behavior of elastic waves is closely linked to a material's microstructure, which governs the interaction of stress and strain gradients under dynamic loading. The formation of solitary waves may also be influenced by geometric effects in the mathematical model. Consequently, introducing a mathematical model to study the effect of geometric nonlinearity on wave propagation should involve higher–order strain gradients, such as the dilatation gradient vector, deviatoric stretch gradient tensor, and symmetric rotation gradient tensor, which give rise to nonlocal effects that significantly affect the waves dispersion and attenuation. Moreover, the inclusion of nonlinearity into the strain tensor and its gradients and the use of variational principles may lead to new wave responses, such as kink and anti-kink waves, soliton and anti–soliton waves, and dark–bright and bright–dark waves.

Other waves known as the *dromion* and *anti–dromion*, can be obtained for the nonlinear partial differential equation (NPDE) using the Darboux transformation [18]. These waves constitute a class of localized solutions characterized by their exponential decay in all spatial directions. Applying the Darboux transformation involves several steps. One begins with a known solution of the PDE, often a trivial or simple one, referred to as the *seed solution*. The transformation then employs this seed solution to generate a new, more complex solution. This procedure typically requires solving auxiliary linear problems associated with the original nonlinear equation, known as lax pairs. By modifying these linear problems, the Darboux transformation produces new solutions that exhibit rich physical and mathematical properties.

This work follows a similar direction, where we investigate the effects of nonlinearity induced by geometric terms in the strain tensor. The strain tensor and its gradient are decomposed into the dilatation gradient vector, deviatoric stretch gradient tensor, and symmetric rotation gradient tensor. By applying the variational principle, we derive the field equations, boundary conditions, and constitutive relations. Therefore, the paper is organized as follows: Section 2 is devoted to applying the variational principle to the strain energy functional and the virtual work of external forces. In this section, a general mathematical formulation is introduced to derive the governing equations. The strain energy functional is defined, and the corresponding field equations, boundary conditions, and constitutive relations are obtained. Section 3 presents a one–dimensional formulation of the mathematical model. In Section 4, wave solutions under various initial and boundary conditions are examined. Section 5 provides numerical simulations and discussions. Finally, Section 6 presents the conclusions of the study.

2. Variational principle

Let an elastic body occupy a volume V, bounded by a surface S. When this body is subjected to large external forces, the resulting deformation may be substantial, rendering the linearized strain measures

insufficient to capture the mechanical response accurately. In such cases, it becomes necessary to employ a nonlinear strain measure that accounts for large deformation. The Green–Lagrange strain tensor is commonly used for this purpose and is defined as follows:

$$\varepsilon_{(ij)} = \frac{1}{2}\left(u_{i,j} + u_{j,i} + u_{k,i}u_{k,j}\right), \tag{2.1}$$

where $u_i, i = 1, 2, 3$ are the components of the displacement field. The nonlinear term represents the nonlinear deformation, which arises due to the geometry of the domain, and is also measured from the reference configuration of the medium.

Recent advancements in continuum mechanics have led to the development of theoretical frameworks that extend the classical strain tensor, as represented in Eq (2.1). These frameworks incorporate derivatives of the strain tensor as additional measures to investigate interactions between material points at the nano–scale. Such behaviors are often not accurately captured by classical elasticity theories, necessitating the adoption of more refined models. In these extended theories, the gradient of the strain tensor is a critical component, which can be decomposed into two parts: a linear part that accounts for linear deformation, and a nonlinear part that captures complex interactions and higher–order effects at the nano–scale. Therefore, one can write the gradient of strain tensor as follows:

$$\eta_{i(jk)} = \frac{1}{2}\left(u_{j,ki} + u_{k,ji} + u_{m,ji}u_{m,k} + u_{m,j}u_{m,ki}\right), \tag{2.2}$$

where the circular bracket represents the symmetry in the two indices when they are interchangeable. Based on the work of Lam et al. [14], the gradient of the strain tensor $\eta_{i(jk)}$, Eq (2.2), is written in the following form:

$$\begin{aligned}
\gamma_i &= \varepsilon_{mm,i}, \qquad \chi_{(ij)} = \frac{1}{2}\left(e_{ipq}\varepsilon_{qj,p} + e_{jpq}\varepsilon_{qi,p}\right), && (2.3)\\
\eta^{(1)}_{i(jk)} &= \frac{1}{3}\left(\varepsilon_{jk,i} + \varepsilon_{ki,j} + \varepsilon_{ij,k}\right) - \frac{1}{15}\delta_{ij}\left(\varepsilon_{mm,k} + 2\varepsilon_{mk,m}\right)\\
&\quad -\frac{1}{15}\delta_{ki}\left(\varepsilon_{mm,j} + 2\varepsilon_{mj,m}\right) - \frac{1}{15}\delta_{jk}\left(\varepsilon_{mm,i} + 2\varepsilon_{mi,m}\right), && (2.4)
\end{aligned}$$

where γ_i is the dilatation gradient vector, $\eta^{(1)}_{i(jk)}$ is the deviatoric stretch gradient tensor, $\chi_{(ij)}$ is the symmetric rotation gradient tensor and δ_{ij} and e_{ijk} are the Kronecker delta and the alternate tensor, respectively.

Using Eqs (2.1) and (2.2), and with some mathematical manipulation, Eq (2.3) can be expressed in terms of the displacement fields as follows:

$$\begin{aligned}
\gamma_i &= u_{m,mi} + u_{k,m}u_{k,mi}, && (2.5)\\
\eta^{(1)}_{i(jk)} &= \Sigma^{(1)}_{ijkabc}u_{a,bc} + \Sigma^{(2)}_{ijkabc}u_{s,a}u_{s,bc}, && (2.6)\\
\chi_{(ij)} &= \Omega_{ijabc}\left(u_{a,bc} + u_{s,a}u_{s,bc}\right), && (2.7)
\end{aligned}$$

with

$$\Sigma^{(1)}_{ijkabc} = \frac{1}{3}\Big[\delta_{aj}\delta_{ib}\delta_{kc} + \delta_{ak}\delta_{ib}\delta_{jc} + \delta_{ai}\delta_{jb}\delta_{ck} - \frac{2}{5}\left(\delta_{jk}\delta_{ic}\delta_{ab} + \delta_{ki}\delta_{jc}\delta_{ab} + \delta_{ij}\delta_{ab}\delta_{kc}\right) - \frac{1}{5}\delta_{bc}\left(\delta_{ij}\delta_{ka} + \delta_{jk}\delta_{ia} + \delta_{ki}\delta_{ja}\right)\Big], \tag{2.8}$$

$$\Sigma^{(2)}_{ijkabc} = \frac{1}{3}\Big[\delta_{ib}\delta_{jc}\delta_{ak} + \delta_{ib}\delta_{kc}\delta_{ja} + \delta_{jb}\delta_{kc}\delta_{ai} - \frac{1}{5}\delta_{ij}\left(2\delta_{kc}\delta_{ab} + \delta_{ak}\delta_{bc}\right) - \frac{2}{5}\left(\delta_{jk}\delta_{bi}\delta_{ac} + \delta_{ki}\delta_{jb}\delta_{ac}\right) - \frac{1}{5}\delta_{bc}\left(\delta_{jk}\delta_{ai} + \delta_{ki}\delta_{aj}\right)\Big], \tag{2.9}$$

$$\Omega_{ijabc} = \frac{1}{4}\Big[\delta_{jb}e_{ica} + \delta_{ib}e_{jca} + \delta_{ja}e_{icb} + \delta_{ia}e_{jcb}\Big]. \tag{2.10}$$

The variational principle, as referenced in [19–21], is a cornerstone methodology in both physics and engineering disciplines. It provides a systematic approach for deriving the fundamental equations that describe the behavior of dynamical systems, as well as the boundary conditions necessary for their unique and physically meaningful solutions. This principle is particularly significant because it offers a unified framework for understanding diverse physical phenomena through a common mathematical foundation.

$$\int_{t_1}^{t_2} \delta\widetilde{\mathcal{W}}^{in} dt = \int_{t_1}^{t_2} \delta\mathcal{W}^{ex} dt + \int_{t_1}^{t_2} \delta\mathcal{T}\, dt, \tag{2.11}$$

where $\widetilde{\mathcal{W}}^{in}$ represents the strain energy functional per unit of volume; $\mathcal{W}^{ex}$ denotes the work done by external forces per unit of volume or per unit surface, depending on the type of acting forces; and $\mathcal{T}$ is the kinetic energy per unit of volume. The strain energy functional for the entire volume of the elastic body, $\widetilde{\mathcal{W}}^{in}$, is considered a function of nonlinear strain tensor, (Eq (2.1)), the dilatation gradient vector (Eq (2.5)), the deviatoric stretch gradient tensor, (Eq (2.6)), and the symmetric rotation gradient tensor, (Eq (2.7)). Therefore, we have:

$$\widetilde{\mathcal{W}}^{in} = \int_V \mathcal{W}^{in}\left(\varepsilon_{(ij)}, \pi_i, \eta^{(1)}_{i(jk)}, \chi_{(ij)}\right) dV. \tag{2.12}$$

The variation of the strain energy functional is defined as follows:

$$\delta\widetilde{\mathcal{W}}^{in} = \int_V \left(\frac{\partial\mathcal{W}^{in}}{\partial\varepsilon_{(ij)}}\delta\varepsilon_{ij} + \frac{\partial\mathcal{W}^{in}}{\partial\gamma_i}\delta\gamma_i + \frac{\partial\mathcal{W}^{in}}{\partial\eta^{(1)}_{i(jk)}}\delta\eta^{(1)}_{i(jk)} + \frac{\partial\mathcal{W}^{in}}{\chi_{(ij)}}\delta\chi_{(ij)}\right) dV. \tag{2.13}$$

Let us introduce the constitutive relations by the following relations

$$\sigma_{ij} = \frac{\partial\mathcal{W}^{in}}{\partial\varepsilon_{(ij)}}, \qquad \pi_i = \frac{\partial\mathcal{W}^{in}}{\partial\gamma_i} \qquad \tau^{(1)}_{i(jk)} = \frac{\partial\mathcal{W}^{in}}{\partial\eta^{(1)}_{i(jk)}}, \qquad m_{(ij)} = \frac{\partial\mathcal{W}^{in}}{\chi_{(ij)}}, \tag{2.14}$$

where σ_{ij}, π_i, $\tau^{(1)}_{i(jk)}$, and $m^{(S)}_{(ij)}$ represent the stresses conjugated to the set of strains metrics $\varepsilon_{(ij)}$, γ_i, $\eta^{(1)}_{i(jk)}$, and $\chi_{(ij)}$, respectively.

Therefore, by substituting Eq (2.14) into Eq (2.13), the equation takes the following form:

$$\delta\widetilde{\mathcal{W}}^{in} = \int_V \left(\sigma_{(ij)}\delta\varepsilon_{(ij)} + \pi_i\delta\gamma_i + \tau^{(1)}_{i(jk)}\delta\eta^{(1)}_{i(jk)} + m_{(ij)}\delta\chi_{(ij)}\right)dV, \tag{2.15}$$

where the variation in strain tensor is

$$\delta\varepsilon_{(ij)} = \Sigma^{(0)}_{ijab}\left(\delta u_{a,b} + u_{k,b}\delta u_{k,a}\right), \tag{2.16}$$

with

$$\Sigma^{(0)}_{ijab} = \frac{1}{2}\left(\delta_{ia}\delta_{jb} + \delta_{ib}\delta_{ja}\right).$$

The variations of the dilatation gradient vector, the deviatoric stretch gradient tensor, and the symmetric rotation gradient tensor are expressed in the following form:

$$\begin{aligned}
\delta\gamma_i &= u_{k,mi}\delta u_{k,m} + \left(\delta_{ab}\delta_{ic} + \delta_{ic}u_{a,b}\right)\delta u_{a,bc}, &(2.17)\\
\delta\eta^{(1)}_{i(jk)} &= \Sigma^{(2)}_{ijkabc}u_{s,bc}\delta u_{s,a} + \left(\Sigma^{(1)}_{ijkabc} + \Sigma^{(2)}_{ijkqbc}u_{a,q}\right)\delta u_{a,bc}, &(2.18)\\
\delta\chi_{(ij)} &= \Omega_{ijabc}\left(u_{s,bc}\delta u_{s,a} + \left(\delta u_{a,bc} + u_{s,a}\delta u_{s,bc}\right)\right). &(2.19)
\end{aligned}$$

By substituting Eqs (2.16)–(2.19) into Eq (2.15), the equation takes the following form:

$$\delta\widetilde{\mathcal{W}}^{in} = \int_V \left(\Pi^{(1)}_{sa}\delta u_{s,a} + \Pi^{(2)}_{abc}\delta u_{a,bc}\right)dV, \tag{2.20}$$

with

$$\Pi^{(1)}_{sa} = \Sigma^{(0)}_{ijsa}\sigma_{(ij)} + \Sigma^{(0)}_{ijab}\sigma_{(ij)}u_{s,b} + \pi_i u_{s,ai} + \tau^{(1)}_{i(jk)}\Sigma^{(2)}_{ijkabc}u_{s,bc} + \Omega_{ijabc}m_{(ij)}u_{s,bc}, \tag{2.21}$$

$$\Pi^{(2)}_{abc} = \delta_{ab}\pi_c + \pi_c u_{a,b} + \tau^{(1)}_{i(jk)}\Sigma^{(1)}_{ijkabc} + \Omega_{ijabc}m_{(ij)} + \tau^{(1)}_{i(jk)}\Sigma^{(2)}_{ijkqbc}u_{a,q} + \Omega_{ijqbc}m_{(ij)}u_{a,q}. \tag{2.22}$$

Use the following relations:

$$\begin{aligned}
\Pi^{(1)}_{sa}\delta u_{s,a} &= \left(\Pi^{(1)}_{sa}\delta u_s\right)_{,a} - \Pi^{(1)}_{sa,a}\delta u_s,\\
\Pi^{(2)}_{abc}\delta u_{a,bc} &= \left(\Pi^{(2)}_{abc}\delta u_{a,b}\right)_{,c} - \left(\Pi^{(2)}_{abc,c}\delta u_a\right)_{,b} + \Pi^{(2)}_{abc,bc}\delta u_a.
\end{aligned}$$

Therefor, Eq (2.20) after using the divergence theorem takes the following form:

$$\delta\widetilde{\mathcal{W}}^{in} = -\int_V \Pi^{Ph}_{ab,b}\delta u_a dV + \int_S n_b\Pi^{Ph}_{ab}\delta u_a dS + \int_S n_c\Pi^{(2)}_{abc}\delta u_{a,b}dS, \tag{2.23}$$

where we use the following substitution:

$$\Pi^{Ph}_{ab} = \Pi^{(1)}_{ab} - \Pi^{(2)}_{abc,c}. \tag{2.24}$$

The work done by the external body forces and surface traction force, higher traction force, and wedge force are defined by

$$\int_V \mathcal{W}^{ex}dV = \int_V f^{ex}_i u_i dV + \int_S \left(t^{ex}_i u_i + \tau^{ex}_i n_j u_{i,j}\right)dS + \int_{\partial S} F^{\text{edge}}_i u_i dL, \tag{2.25}$$

where f_i^{ex} is the external body force per unit of volume, t_i^{ex} is the external traction vector per unit surface, τ_i^{ex} represents the higher-order traction vector per unit of surface, acting in the direction of the normal to that surface, and F_i^{edge} is the wedge force per unit of length.

The variation of the work done by external forces are given by

$$\int_V \delta \mathcal{W}^{ex} dV = \int_V f_i^{ex} \delta u_i dV + \int_S \left(t_i^{ex} \delta u_i + \tau_i^{ex} n_j \delta u_{i,j} \right) dS + \int_{\partial S} F_i^{\text{edge}} \delta u_i dL. \tag{2.26}$$

The total kinetic energy for the entire material includes the micro–inertia effect is defined by:

$$\mathcal{T} = \frac{1}{2}\rho \int_V \dot{u}_j \dot{u}_j dV + \frac{1}{2}\rho h^2 \int_V \dot{u}_{i,j} \dot{u}_{i,j} dV, \tag{2.27}$$

where ρ is a mass density and h is the internal length–scale parameter corresponding to the micro–inertia effect.

The variation principle for the kinetic energy with micro–inertia term gives as follows:

$$\delta \mathcal{T} = \int_V \rho \dot{u}_j \delta \dot{u}_j dV + \rho h^2 \int_V \dot{u}_{i,j} \delta \dot{u}_{i,j} dV, \tag{2.28}$$

by using the following property:

$$\dot{u}_{i,j} \delta \dot{u}_{i,j} = \left(\dot{u}_{i,j} \delta \dot{u}_i \right)_{,j} - \dot{u}_{i,jj} \delta \dot{u}_i.$$

Finally, the variation for the kinetic energy is written as follows:

$$\delta \mathcal{T} = \int_V \rho \left(\dot{u}_i - h^2 \dot{u}_{i,jj} \right) \delta \dot{u}_i dV + \rho h^2 \int_V \left(\dot{u}_{i,j} \delta \dot{u}_i \right)_{,j} dV. \tag{2.29}$$

If we use the divergence theorem for the last term in Eq (2.29), then

$$\delta \mathcal{T} = \int_V \rho \left(\dot{u}_i - h^2 \dot{u}_{i,jj} \right) \delta \dot{u}_i dV + \rho h^2 \int_S n_j \dot{u}_{i,j} \delta \dot{u}_i dS. \tag{2.30}$$

Substituting from Eqs (2.20), (2.26), and (2.30) into Eq (2.11), we have

$$\begin{aligned} \int_{t_1}^{t_2} \Big(& - \int_V \left(\Pi_{ij,j}^{\text{Ph}} + f_i^{\text{ex}} \right) \delta u_i \, dV - \int_S \left(t_i^{\text{ex}} - n_j \Pi_{ij}^{\text{Ph}} \right) \delta u_i \, dS - \int_S \tau_i^{\text{ex}} n_j \delta u_{i,j} \, dS \\ & + \int_S n_c \Pi_{abc}^{(2)} \delta u_{a,b} \, dS - \int_{\partial S} F_i^{\text{edge}} \delta u_i \, dL - \rho \int_V \left(\dot{u}_i - h^2 \dot{u}_{i,jj} \right) \delta \dot{u}_i \, dV \\ & - \rho h^2 \int_S n_j \dot{u}_{i,j} \delta \dot{u}_i \, dS \Big) dt = 0. \end{aligned} \tag{2.31}$$

Integrate by parts for the last two terms of Eq (2.31) as follows:

$$\int_{t_1}^{t_2} \int_V \left(\dot{u}_i - h^2 \dot{u}_{i,jj} \right) \delta \dot{u}_i dt = - \int_{t_1}^{t_2} \int_V \left(\ddot{u}_i - h^2 \ddot{u}_{i,jj} \right) \delta u_i dV dt, \tag{2.32}$$

$$\int_{t_1}^{t_2}\int_{S}\left(n_j\dot{u}_{i,j}\delta\dot{u}_i\right)dS\,dt = -\int_{t_1}^{t_2}\int_{S} n_j\ddot{u}_{i,j}\delta u_i dS\,dt. \tag{2.33}$$

Finally, by substituting from Eqs (2.32) and (2.33) into Eq (2.31), we have

$$\int_{t_1}^{t_2}\Bigg(-\int_{V}\left(\Pi^{Ph}_{ij,j}+f^{ex}_i-\rho\ddot{u}_i+\rho h^2\ddot{u}_{i,jj}\right)\delta u_i dV-\int_{S}\left(t^{ex}_i-n_j\Pi^{Ph}_{ij}-\rho h^2 n_j\ddot{u}_{i,j}\right)\delta u_i dS$$
$$-\int_{S}\tau^{ex}_i n_j\delta u_{i,j}dS+\underline{\int_{S}\Pi^{(2)}_{kji}n_i\delta u_{k,j}dS}-\int_{\partial S}F^{\text{edge}}_i\delta u_i dL\Bigg)dt=0. \tag{2.34}$$

Decompose the Kronecker's delta into the sum of the normal $n_k n_i$ and the tangential operator $\mathcal{N}_{mj}$, as follows:

$$\delta_{mj}=\mathcal{N}_{mj}+n_m n_j, \tag{2.35}$$

one can prove the following identity:

$$\mathcal{N}_{mj}=\mathcal{N}_{ma}\mathcal{N}_{aj},$$

then the underlined term in Eq (2.34) becomes

$$\int_{S}\Pi^{(2)}_{kji}n_i\delta u_{k,j}dS=\int_{S}\left(\Pi^{(2)}_{kji}n_i\mathcal{N}_{aj}\delta u_{k,m}\right)\mathcal{N}_{ma}dS+\int_{S}\left(\Pi^{(2)}_{kji}n_i n_j\right)\delta u_{k,m}n_m dS. \tag{2.36}$$

If we use the following relation:

$$\Pi^{(2)}_{kji}n_i\mathcal{N}_{aj}\delta u_{k,m}=\left(\Pi^{(2)}_{kji}n_i\mathcal{N}_{aj}\delta u_k\right)_{,m}-\left(\Pi^{(2)}_{kji}n_i\mathcal{N}_{aj}\right)_{,m}\delta u_k,$$

then Eq (2.36) is written as follows:

$$\begin{aligned}\int_{S}\Pi^{(2)}_{kji}n_i\delta u_{k,j}dS &= \int_{S}\left(\widetilde{\Phi}_j\mathcal{N}_{aj}\right)_{,m}\mathcal{N}_{ma}dS-\int_{S}\left(\Pi^{(2)}_{kji}n_i\mathcal{N}_{aj}\right)_{,m}\delta u_k\mathcal{N}_{ma}dS\\ &\quad+\int_{S}\left(\Pi^{(2)}_{iqp}n_q n_p\right)\delta u_{i,j}n_j dS,\end{aligned} \tag{2.37}$$

where

$$\widetilde{\Phi}_j=\Pi^{(2)}_{kji}n_i\delta u_k.$$

The divergence theorem, [22, 23], for any vector field $\widetilde{\Phi}_j$ defined in a neighborhood of an embedded Riemannian manifold $\mathcal{M}$

$$\int_{\mathcal{M}}\left(\mathcal{N}_{aj}\widetilde{\Phi}_j\right)_{,m}\mathcal{N}_{ma}dS=\int_{\partial\mathcal{M}}\widetilde{\Phi}_j\mathcal{N}_{jm}\gamma_m dL, \tag{2.38}$$

where γ_j is the unit of the external normal to $\mathcal{M}$ that is defined on its border and belongs to the tangent space to $\mathcal{M}$.

After that, Eq (2.37) takes the following form:

$$\int_S \Pi^{(2)}_{kji} n_i \delta u_{k,j} dS = \int_{\partial \mathcal{M}} \widetilde{\Phi}_j \mathcal{N}_{jm} \gamma_m dL - \int_S \left(\Pi^{(2)}_{kji} n_i \mathcal{N}_{aj} \right)_{,m} \mathcal{N}_{ma} \delta u_k dS + \int_S \left(\Pi^{(2)}_{iqp} n_q n_p \right) \delta u_{i,j} n_j dS. \tag{2.39}$$

By substituting Eq (2.39) into Eq (2.34), one can obtain

$$\int_{t_1}^{t_2} \Bigg(- \int_V \left(\Pi^{Ph}_{ij,j} + f^{ex}_i - \rho \ddot{u}_i + \rho h^2 \ddot{u}_{i,jj} \right) \delta u_i dV - \int_S \left(t^{ex}_i - n_j \Pi^{Ph}_{ij} - \rho h^2 n_j \ddot{u}_{i,j} + \left(\Pi^{(2)}_{ijk} n_k \mathcal{N}_{aj} \right)_{,m} \mathcal{N}_{ma} \right) \delta u_i dS - \int_S \left(\tau^{ex}_i - \Pi^{(2)}_{iqp} n_q n_p \right) n_j \delta u_{i,j} dS - \int_{\partial S} \left(F^{\text{edge}}_k - \Pi^{(2)}_{kji} n_i \mathcal{N}_{jm} \gamma_m \right) \delta u_k dL \Bigg) dt = 0. \tag{2.40}$$

Finally, the Hamiltonian principle leads to all the integrands vanishing. These produce the field equations

$$\Pi^{Ph}_{ij,j} + f^{ex}_i = \rho \ddot{u}_i - \rho h^2 \ddot{u}_{i,jj}, \qquad \forall x \in V, \tag{2.41}$$

and the boundary conditions

$$t^{ex}_i = n_j \left(\Pi^{Ph}_{ij} + \rho h^2 \ddot{u}_{aj} \right)_{,m} \mathcal{N}_{ma}, \tag{2.42}$$

$$\tau^{ex}_i = \Pi^{(2)}_{iqp} n_q n_p, \tag{2.43}$$

$$F^{\text{edge}}_k = \Pi^{(2)}_{kji} n_i \mathcal{N}_{jm} \gamma_m. \tag{2.44}$$

According to [14], the total strain energy density functional is defined as a function of several internal variables that describe the material's deformation. These include the classical symmetric strain tensor, $\varepsilon_{(ij)}$, which quantifies the deformation; the dilatation gradient vector, γ_i, which represents changes in volume; the deviatoric stretch gradient tensor, $\eta^{(1)}_{i(jk)}$, which measures the shape changes; and the symmetric rotation gradient tensor, $\chi_{(ij)}$, which accounts for rotational effects. Therefore, one can write

$$\widetilde{\mathcal{W}}^{in} = \widetilde{\mathcal{W}}^{in} \left(\varepsilon_{ij}, \gamma_i, \eta^{(1)}_{ijk}, \chi^{(S)}_{ij} \right).$$

Since we are interested in studying nonlinear behavior caused by geometric deformation and are not including nonlinearity due to the material properties, the strain energy functional for isotropic elastic materials is chosen to be in quadratic form as follows:

$$\widetilde{\mathcal{W}}^{in} \left(\varepsilon_{(ij)}, \gamma_i, \eta^{(1)}_{i(jk)}, \chi_{(ij)} \right) = \frac{1}{2} \lambda \varepsilon_{ii} \varepsilon_{jj} + \mu \varepsilon'_{(ij)} \varepsilon'_{(ij)} + a'_0 \gamma_i \gamma_i + a'_1 \eta^{(1)}_{ijk} \eta^{(1)}_{ijk} + a'_2 \chi_{(ij)} \chi_{(ij)}, \tag{2.45}$$

where ε'_{ij} is the deviatoric strain, which is defined by the following relation:

$$\varepsilon'_{ij} = \varepsilon_{ij} - \frac{1}{3} \delta_{ij} \varepsilon_{mm}, \tag{2.46}$$

where κ and μ represent the bulk and shear moduli, respectively, and a'_n, $n = 0, 1, 2$, are the additional independent material parameters related to dilatation gradients, deviatoric stretch gradients, and rotation gradients, respectively.

Choose the independent material parameters a'_n, $n = 0, 1, 2$ as follows:

$$a'_0 = \mu l_0^2, \qquad a'_1 = \mu l_1^2, \qquad a'_2 = \mu l_2^2,$$

where l_0, l_1, and l_2 are three material length–scale parameters.

The constitutive relations can be derived by substituting the expression of the deformation energy density functional from Eq (2.45) into Eq (2.14), which yields the desired results

$$\sigma_{ij} = \lambda\delta_{ij}\varepsilon_{mm} + 2\mu\varepsilon'_{ij} - \frac{2}{3}\mu\delta_{ij}\left(1 - \frac{1}{3}\delta_{qq}\right)\varepsilon_{mm}, \tag{2.47}$$

$$\pi_i = 2\mu l_0^2\gamma_i, \tag{2.48}$$

$$\tau^{(1)}_{i(jk)} = 2\mu l_1^2\eta^{(1)}_{i(jk)}, \tag{2.49}$$

$$m_{(ij)} = 2\mu l_2^2\chi_{(ij)} \tag{2.50}$$

where

$$\delta_{qq} = \begin{cases} 1, & q = 1, \\ 2, & q = 1, 2, \\ 3, & q = 1, 2, 3. \end{cases}$$

It is important to note that the theory presented by Lam et al. [14] involves only three length scale parameters. Furthermore, when addressing boundary value problems in one or two dimensions, the last term in the classical stress tensor σ_{ij}, Eq (2.47) is neglected in the theory. while this term vanishes only in three-dimensions.

Therefore, the stresses σ_{ij}, π_i, $\tau^{(1)}_{i(jk)}$, and $m_{(ij)}$ can be expressed in terms of the displacement field by using Eqs (2.1), (2.5)–(2.7) as follows:

$$\sigma_{ij} = \delta^{(1)}_{ijab}u_{a,b} + \delta^{(2)}_{ijab}u_{k,a}u_{k,b}, \tag{2.51}$$

$$\pi_i = 2\mu l_0^2\left(u_{m,mi} + u_{k,m}u_{k,mi}\right), \tag{2.52}$$

$$\tau^{(1)}_{i(jk)} = 2\mu l_1^2\left(\Sigma^{(1)}_{ijkabc}u_{a,bc} + \Sigma^{(2)}_{ijkabc}u_{s,a}u_{s,bc}\right), \tag{2.53}$$

$$m_{(ij)} = 2\mu l_2^2\Omega_{ijabc}\left(u_{a,bc} + u_{s,a}u_{s,bc}\right) \tag{2.54}$$

with

$$\delta^{(1)}_{(ij)ab} = \delta_{ij}\delta_{ab}\left(\lambda - \frac{4}{3}\mu + \frac{2}{9}\mu\delta_{qq}\right) + \mu\left(\delta_{ia}\delta_{jb} + \delta_{ib}\delta_{ja}\right), \tag{2.55}$$

$$\delta^{(2)}_{ijab} = \left(\frac{\lambda}{2} - \frac{\mu}{3}\right)\delta_{ij}\delta_{ab} + \mu\delta_{ia}\delta_{jb} - \frac{1}{3}\mu\delta_{ij}\delta_{ab}\left(1 - \frac{1}{3}\delta_{qq}\right). \tag{2.56}$$

In the following, the quantities listed in Eqs (2.21), (2.22), and (2.24) are expressed in terms of the displacement fields with the help of Eqs (2.51)–(2.54) as follows:

$$\Pi^{(1)}_{sa} = \delta^{(1)}_{asqp}u_{q,p} + \Gamma^{(1)}_{sakbqp}u_{k,b}u_{q,p} + \Gamma^{(2)}_{abcpqk}u_{s,bc}u_{p,qk}, \tag{2.57}$$

$$\Pi^{(2)}_{abc} = \Gamma^{(3)}_{abcpql} u_{p,ql} + \Gamma^{(4)}_{abcrmpql} u_{r,m} u_{p,ql} \tag{2.58}$$

with

$$\Gamma^{(1)}_{sakbqp} = \delta_{sk}\delta^{(1)}_{abqp} + \frac{1}{2}\delta_{kq}\left(\delta^{(2)}_{sapb} + \delta^{(2)}_{aspb}\right), \tag{2.59}$$

$$\Gamma^{(2)}_{abcpqk} = 2\mu\left(l_0^2\delta_{ab}\delta_{qp}\delta_{ck} + l_2^2\Omega_{ijabc}\Omega_{ijpqk} + l_1^2\Sigma^{(1)}_{ijmpqk}\Sigma^{(2)}_{ijmabc}\right), \tag{2.60}$$

$$\Gamma^{(3)}_{abcpql} = 2\mu\left(l_0^2\delta_{ab}\delta_{pq}\delta_{cl} + l_2^2\Omega_{ijabc}\Omega_{ijpql} + l_1^2\Sigma^{(1)}_{ijkabc}\Sigma^{(1)}_{ijkpql}\right), \tag{2.61}$$

$$\begin{aligned}\Gamma^{(4)}_{abcrmpql} = 2\mu\Big[&l_0^2\left(\delta_{ab}\delta_{cl}\delta_{qm}\delta_{pr} + \delta_{cl}\delta_{pq}\delta_{bm}\delta_{ar}\right)\\ &+ l_1^2\left(\delta_{pr}\Sigma^{(1)}_{ijkabc}\Sigma^{(2)}_{ijkmql} + \delta_{ar}\Sigma^{(1)}_{ijkpql}\Sigma^{(2)}_{ijkmbc}\right)\\ &+l_2^2\left(\delta_{pr}\Omega_{ijmql}\Omega_{ijabc} + \delta_{ar}\Omega_{ijpql}\Omega_{ijmbc}\right)\Big].\end{aligned} \tag{2.62}$$

Furthermore, Eq (2.24) can be expressed in terms of the displacement fields as follows:

$$\Pi^{Ph}_{ab} = \delta^{(1)}_{baqp}u_{q,p} - \Gamma^{(3)}_{abcpql}u_{p,qlc} + \Gamma^{(1)}_{abkrqp}u_{k,r}u_{q,p} + \Gamma^{(5)}_{abcnmpqk}u_{n,mc}u_{p,qk} - \Gamma^{(4)}_{abcrmpql}u_{r,m}u_{p,qlc}, \tag{2.63}$$

with

$$\Gamma^{(5)}_{abcnmpqk} = \delta_{an}\Gamma^{(2)}_{bmcpqk} - \Gamma^{(4)}_{abcnmpqk}. \tag{2.64}$$

Now, after determining the constitutive relations in terms of the displacement fields from the strain energy functional, we will obtain the field equations and the boundary conditions in terms of the displacement field by inserting Eq (2.63) into Eq (2.41)

$$\begin{aligned}&\delta^{(1)}_{jiqp}u_{q,pj} - \Gamma^{(3)}_{ijcpql}u_{p,qlcj} + \Lambda^{(1)}_{ijamkr}u_{k,r}u_{a,jm} + \Lambda^{(2)}_{ijsmpqkl}u_{s,jm}u_{p,qkl}\\ &\quad - \Gamma^{(4)}_{ijcrmpql}u_{r,m}u_{p,qlcj} + f^{ex}_i = \rho\ddot{u}_i - \rho h^2\ddot{u}_{i,jj},\end{aligned} \tag{2.65}$$

with

$$\Lambda^{(1)}_{ijamkr} = \Gamma^{(1)}_{ijamkr} + \Gamma^{(1)}_{ijkram}, \qquad \Lambda^{(2)}_{ijsmpqkl} = \Gamma^{(5)}_{iqlpksjm} + \Gamma^{(5)}_{iljsmpqk} - \Gamma^{(4)}_{ijlsmpqk},$$

and the boundary conditions are written by using Eq (2.22) as follows:

$$\begin{aligned}t^{ex}_i = n_j\Big(&\delta^{(1)}_{jiqp}u_{q,p} - \Gamma^{(3)}_{ijcpql}u_{p,qlc} + \Gamma^{(1)}_{ijkrqp}u_{k,r}u_{q,p}\\ &+ \Gamma^{(5)}_{ijcnmpqk}u_{n,mc}u_{p,qk} - \Gamma^{(4)}_{ijcrmpql}u_{r,m}u_{p,qlc} + \rho h^2\ddot{u}_{i,j}\Big)\\ &- \left(\left(\Gamma^{(3)}_{ijkpql}u_{p,ql} + \Gamma^{(4)}_{ijkrmpql}u_{r,m}u_{p,ql}\right)n_k\mathcal{N}_{aj}\right)_{,s}\mathcal{N}_{sa}, \qquad \forall x \in S_T,\end{aligned} \tag{2.66}$$

$$\tau^{ex}_i = \left(\Gamma^{(3)}_{ijkpql}u_{p,ql} + \Gamma^{(4)}_{ijkrmpql}u_{r,m}u_{p,ql}\right)n_jn_k, \qquad \forall x \in S_T, \tag{2.67}$$

$$F^{\text{edge}}_i = \left(\Gamma^{(3)}_{ijkpql}u_{p,ql} + \Gamma^{(4)}_{ijkrmpql}u_{r,m}u_{p,ql}\right)n_k\mathcal{N}_{js}\gamma_s, \qquad \forall x \in S_T. \tag{2.68}$$

3. Formulation of the problem

Let us consider a semi–infinite, one-dimensional plane occupied by an elastic medium with cubic symmetry. The domain is represented by $x \geq 0$, where $x = 0$ serves as the boundary. Therefore, the displacement field due to the external action is represented by

$$u(x,t) \equiv u_1(x,t).$$

Therefore, the strain tensor, the dilatation gradient vector, the deviatoric stretch gradient tensors and the symmetric rotation gradient tensor (Eqs (2.5)–(2.7)), takes the following form:

$$\gamma_1 = \frac{\partial^2 u}{\partial x^2} + \frac{\partial u}{\partial x}\frac{\partial^2 u}{\partial x^2}, \qquad \eta^{(1)}_{111} = \frac{2}{5}\frac{\partial^2 u}{\partial x^2} + \frac{2}{5}\frac{\partial u}{\partial x}\frac{\partial^2 u}{\partial x^2}, \qquad \chi_{11} = 0, \tag{3.1}$$

where Eqs (2.8)–(2.10) lead to

$$\Sigma^{(1)}_{111111} = \frac{2}{5}, \qquad \Sigma^{(2)}_{111111} = \frac{2}{5}, \qquad \Omega_{11111} = 0.$$

Then Eq (2.65), without considering external force, takes the form

$$\alpha\frac{\partial^2 u}{\partial x^2} - \beta\frac{\partial^4 u}{\partial x^4} + 3\alpha\frac{\partial u}{\partial x}\frac{\partial^2 u}{\partial x^2} - 4\beta\frac{\partial^2 u}{\partial x^2}\frac{\partial^3 u}{\partial x^3} - 2\beta\frac{\partial u}{\partial x}\frac{\partial^4 u}{\partial x^4} = \rho\frac{\partial^2}{\partial t^2}\left(u - h^2\frac{\partial^2 u}{\partial x^2}\right), \tag{3.2}$$

with

$$\alpha = \lambda + \frac{8}{9}\mu, \qquad \beta = 2\mu l_0^2\left(1 + \frac{4}{25}\frac{l_1^2}{l_0^2}\right),$$

where the dimensions of α and β are N/m^2 and N, respectively.

Equation (3.2) represents an extension of the Boussinesq-type equation, which is used to describe the nonlinear behavior of wave propagation in isotropic elastic materials based on the modified strain gradient theory of elasticity introduced by Lam and co-authors. Moreover, Eq (3.2) is identical to the NPDE obtained in [24] by the same author.

The constitutive relations, as given by Eqs (2.51)–(2.54) , take the form:

$$\sigma_{11} = \alpha\left(1 + \frac{1}{2}\frac{\partial u}{\partial x}\right)\frac{\partial u}{\partial x}, \tag{3.3}$$

$$\pi_1 = 2\mu l_0^2\left(1 + \frac{\partial u}{\partial x}\right)\frac{\partial^2 u}{\partial x^2}, \tag{3.4}$$

$$\tau^{(1)}_{111} = \frac{4}{5}\mu l_1^2\left(1 + \frac{\partial u}{\partial x}\right)\frac{\partial^2 u}{\partial x^2}, \tag{3.5}$$

$$m_{11} = 0. \tag{3.6}$$

The boundary conditions, (2.66)–(2.68), are written in the following form:

$$t^{ex} = \alpha\frac{\partial u}{\partial x} - \beta\frac{\partial^3 u}{\partial x^3} + \frac{3}{2}\alpha\left(\frac{\partial u}{\partial x}\right)^2 - \beta\left(\frac{\partial^2 u}{\partial x^2}\right)^2 - 2\beta\frac{\partial u}{\partial x}\frac{\partial^3 u}{\partial x^3} + \rho h^2\frac{\partial^2}{\partial t^2}\left(\frac{\partial u}{\partial x}\right), \tag{3.7}$$

$$\tau^{ex} = \beta\left(1 + 2\frac{\partial u}{\partial x}\right)\frac{\partial^2 u}{\partial x^2}, \tag{3.8}$$

where the notation t^{ex} and τ^{ex}, are used instead of t_1^{ex} and τ_1^{ex} respectively, to avoid ambiguity.

We use the following dimensionless analysis:

$$u^* = \frac{u}{l_0}, \qquad \frac{\partial^2}{\partial t^2} = \frac{1}{t_0^2}\frac{\partial^2}{\partial t^{*2}}, \qquad \frac{\partial^n}{\partial x^n} = \frac{1}{l_0^n}\frac{\partial^n}{\partial x^{*n}},$$

$$t_0 = \sqrt{\frac{\rho l_0^2}{\alpha}}, \qquad \sigma_{11}^* = \frac{\sigma_{11}}{\alpha}, \qquad \pi_1^* = \frac{\pi_1}{\alpha l_0}, \qquad \tau_{111}^* = \frac{\tau_{111}^{(1)}}{\alpha l_0}.$$

Henceforth, the asterisks are omitted to avoid confusion thereby, the field equation takes the form

$$\frac{\partial^2 u}{\partial x^2} - \varkappa \frac{\partial^4 u}{\partial x^4} + 3\frac{\partial u}{\partial x}\frac{\partial^2 u}{\partial x^2} - 4\varkappa \frac{\partial^2 u}{\partial x^2}\frac{\partial^3 u}{\partial x^3} - 2\varkappa \frac{\partial u}{\partial x}\frac{\partial^4 u}{\partial x^4} = \frac{\partial^2 u}{\partial t^2} - \zeta \frac{\partial^4 u}{\partial t^2 \partial x^2}, \tag{3.9}$$

with

$$\varkappa = \frac{\beta}{\alpha l_0^2} > 0, \qquad \zeta = \frac{h^2}{l_0^2} > 0,$$

where $\varkappa$ and ζ without dimension.

The constitutive relations are

$$\sigma_{11} = \left(1 + \frac{1}{2}\frac{\partial u}{\partial x}\right)\frac{\partial u}{\partial x}, \tag{3.10}$$

$$\pi_1 = 2\frac{\mu}{\alpha}\left(1 + \frac{\partial u}{\partial x}\right)\frac{\partial^2 u}{\partial x^2}, \tag{3.11}$$

$$\tau_{111}^{(1)} = \frac{4}{5}\frac{\mu}{\alpha}\frac{l_1^2}{l_0^2}\left(1 + \frac{\partial u}{\partial x}\right)\frac{\partial^2 u}{\partial x^2}, \tag{3.12}$$

$$m_{11} = 0. \tag{3.13}$$

The boundary conditions are

$$t^{ex} = \frac{\partial u}{\partial x} - \varkappa \frac{\partial^3 u}{\partial x^3} + \frac{3}{2}\left(\frac{\partial u}{\partial x}\right)^2 - \varkappa \left(\frac{\partial^2 u}{\partial x^2}\right)^2 - 2\varkappa \frac{\partial u}{\partial x}\frac{\partial^3 u}{\partial x^3} + \zeta \frac{\partial^2}{\partial t^2}\left(\frac{\partial u}{\partial x}\right), \tag{3.14}$$

$$\tau^{ex} = \varkappa\left(1 + 2\frac{\partial u}{\partial x}\right)\frac{\partial^2 u}{\partial x^2}. \tag{3.15}$$

A similar NPDE to (3.9) was introduced in [25], where different material parameters were considered, and it was solved using the exponential reductive perturbation technique (ERPT).

4. The wave solution

Equation (3.9) represents a NPDE that governs wave propagation in an elastic medium, incorporating higher-order spatial and temporal derivatives. The presence of nonlinear terms, along with the mixed high-order derivatives, makes this equation analytically intractable in most general cases. Physically, this NPDE models complex wave phenomena, where the nonlinearity can induce solitary waves, kinks, anti–kinks, solitons, anti–solitons, and bright–dark waves within the microstructure of the medium, as well as bulk waves in the entire material. Due to its complexity, analytical solutions are generally unavailable, and numerical methods are often employed for its solution, though this approach will not be pursued here. Therefore, a wave-like solution is considered below.

Let us assume a wave traveling in the positive x–direction, and proceed to use

$$\xi = k\,(x - \omega t)\,, \qquad\qquad u\,(x,t) = U\,(\xi)\,, \tag{4.1}$$

where ξ represents a wave phase function that describes how a wave propagates in space and time with a wavenumber k and an angular frequency ω.

By substituting from Eq (4.1) into Eq (3.9), we have the following equation:

$$\left(1-\omega^2\right)\frac{d^2U}{d\xi^2}-k^2\left(\varkappa-\zeta\omega^2\right)\frac{d^4U}{d\xi^4}+3k\frac{dU}{d\xi}\frac{d^2U}{d\xi^2}-4\varkappa k^3\frac{d^2U}{d\xi^2}\frac{d^3U}{d\xi^3}-2\varkappa k^3\frac{dU}{d\xi}\frac{d^4U}{d\xi^4}=0. \quad (4.2)$$

It is easy to obtain

$$\left(1-\omega^2\right)\frac{d^2U}{d\xi^2}-k^2\left(\varkappa-\zeta\omega^2\right)\frac{d^4U}{d\xi^4}+\frac{3}{2}k\frac{d}{d\xi}\left(\frac{dU}{d\xi}\right)^2+\varkappa k^3\frac{d}{d\xi}\left(\frac{d^2U}{d\xi^2}\right)^2-\varkappa k^3\frac{d^3}{d\xi^3}\left(\frac{dU}{d\xi}\right)^2=0. \quad (4.3)$$

If we integrate Eq (4.3) with respect to ξ and neglect integration constant, then we have

$$\frac{d^3U}{d\xi^3}-q_0\frac{dU}{d\xi}-q_1\left(\frac{dU}{d\xi}\right)^2-q_2\left(\frac{d^2U}{d\xi^2}\right)^2+q_2\frac{d^2}{d\xi^2}\left(\frac{dU}{d\xi}\right)^2=0, \quad (4.4)$$

with

$$q_0=\frac{1}{k^2}\frac{1-\omega^2}{\varkappa-\zeta\omega^2},\qquad q_1=\frac{3}{2}\frac{1}{k}\frac{1}{\varkappa-\zeta\omega^2},\qquad q_2=\frac{\varkappa k}{\varkappa-\zeta\omega^2}. \quad (4.5)$$

Let us use the following substitutions:

$$W=\frac{dU}{d\xi},\qquad \frac{d^2}{d\xi^2}\left(W^2\right)=2W'^2+2WW'', \quad (4.6)$$

therefore, Eq (4.4) becomes:

$$\left(1+2q_2W\right)W''+q_2W'^2=q_0W+q_1W^2. \quad (4.7)$$

We also use the following substitution

$$\left(1+2q_2W\right)W''+q_2W'^2=\frac{1}{2}\frac{d}{dW}\left[\left(1+2q_2W\right)W'^2\right].$$

Therefore, Eq (4.7) is written as follows:

$$\frac{d}{dW}\left[\left(1+2q_2W\right)W'^2\right]=2q_0W+2q_1W^2. \quad (4.8)$$

If we integrate Eq (4.8) with respect to W and choose the integration constant to be zero, then we can obtain

$$W'^2=\frac{q_0W^2}{1+2q_2W}+\frac{2}{3}\frac{q_1W^3}{1+2q_2W}. \quad (4.9)$$

Use the partial fractional for the right–hand side in Eq (4.9) as follows:

$$W'^2=-A+2q_2AW+\frac{1}{3}\frac{q_1}{q_2}W^2+\frac{A}{1+2q_2W}, \quad (4.10)$$

with

$$A=\frac{1}{4}\frac{1}{q_2^2}\left(q_0-\frac{1}{3}\frac{q_1}{q_2}\right).$$

In the following analysis, Eq (4.10) is examined under the condition that the angular frequency ω is set to unity. Consequently, the associated quantity (Eq (4.5)), takes the following form:

$$q_0 = 0, \qquad q_1 = \frac{3}{2}\frac{1}{k}\frac{1}{\varkappa - \zeta}, \qquad q_2 = \frac{\varkappa k}{\varkappa - \zeta}, \qquad A = -\frac{1}{12}\frac{q_1}{q_2^3}. \tag{4.11}$$

This choice creates two cases for the relation between the material parameters $\varkappa$ and ζ as follows.

Case (1). If $\varkappa - \zeta > 0$, then both q_1 and q_2 are positive and $h < l_0$, l_1, and l_2, therefore, no changes occurs for Eq (4.10), but we stipulate the condition $-1/2q_2 < W < 1/2q_2$ to apply the binomial theorem for the last term in Eq (4.10) and we will stop at the order 4. By substituting into Eq (4.10), and with some mathematical calculation, we reach to the following formula

$$\frac{dW}{W^{3/2}\sqrt{1 - 2q_2 W}} = \sqrt{\frac{2}{3}q_1}d\xi. \tag{4.12}$$

If we integrate with respect to ξ, then we have

$$\int \frac{dW}{W^{3/2}\sqrt{1 - 2q_2 W}} = \sqrt{\frac{2}{3}q_1}\xi + C_1, \tag{4.13}$$

where C_1 is the integration constant.
Integrating the left–hand side of Eq (4.13), we reach the formula:

$$W(\xi) = \frac{1}{2q_2 + \frac{1}{4}\left(\sqrt{\frac{2}{3}q_1}\xi + C_1\right)^2}. \tag{4.14}$$

If we use Eq $(4.6)_1$ and integrate, we derive the following formula:

$$U(\xi) = \int \frac{1}{2q_2 + \frac{1}{4}\left(\sqrt{\frac{2}{3}q_1}\xi + C_1\right)^2}d\xi + C_2, \tag{4.15}$$

where C_2 is the integration constant.
Performing the integration in Eq (4.15), we obtain

$$U(\xi) = \sqrt{\frac{3}{q_1 q_2}}\arctan\left(\sqrt{\frac{1}{12}\frac{q_1}{q_2}}\xi + \frac{C_1}{\sqrt{8q_2}}\right) + C_2. \tag{4.16}$$

If we retrieve the displacement $u(x,t)$, by using Eq (4.1), we obtain

$$u(x,t) = \sqrt{\frac{3}{q_1 q_2}}\arctan\left(\sqrt{\frac{1}{12}\frac{q_1}{q_2}}k(x - t) + \frac{C_1}{\sqrt{8q_2}}\right) + C_2. \tag{4.17}$$

Here, C_1 and C_2 are integration constants determined from the initial and boundary conditions. These conditions are chosen in a suitable way to give three types of wave propagation as follows:

(a) Constant initial and boundary conditions:
The following initial and boundary conditions are used to determine the constants C_1 and C_2 for the displacement field Eq (4.17), as follows:

$$u(0,0) = u_0, \qquad u(x \to \pm\infty, t) = \pm\frac{\pi}{2}\sqrt{\frac{3}{q_1 q_2}}, \tag{4.18}$$

where u_0 is a given displacement constant field; therefore, these two conditions give the following expressions for the two constants C_1 and C_2 as follows:

$$C_1 = \sqrt{8q_2}\tan\left(\sqrt{\frac{q_1 q_2}{3}}u_0\right), \qquad C_2 = 0.$$

Then the displacement takes the form

$$u(x,t) = \sqrt{\frac{3}{q_1 q_2}}\arctan\left(\sqrt{\frac{1}{12}\frac{q_1}{q_2}}k(x-t) + \tan\left(\sqrt{\frac{q_1 q_2}{3}}u_0\right)\right), \tag{4.19}$$

where q_1 and q_2 are defined by Eq (4.11).

(b) Dynamical boundary condition:
The boundary conditions are given in the following way:

$$u(0,t) = f(t), \qquad u(x \to \pm\infty, t) = \pm\frac{\pi}{2}\sqrt{\frac{3}{q_1 q_2}}, \tag{4.20}$$

where $f(t)$ is a given function, therefore, these two conditions give the following expressions for the two constants C_1 and C_2 :

$$C_1(t) = \sqrt{8q_2}\tan\left(\sqrt{\frac{q_1 q_2}{3}}f(t)\right) + k\sqrt{\frac{2}{3}q_1}t, \qquad C_2 = 0.$$

We note here that $C_1(t)$ is a quantity change with time, and thus the displacement takes the form

$$u(x,t) = \sqrt{\frac{3}{q_1 q_2}}\arctan\left(k\sqrt{\frac{1}{12}\frac{q_1}{q_2}}x + \tan\left(\sqrt{\frac{q_1 q_2}{3}}f(t)\right)\right). \tag{4.21}$$

(c) Static initial condition:
The initial condition and boundary conditions are

$$u(x,0) = g(x), \qquad u(x \to \pm\infty, t) = \pm\frac{\pi}{2}\sqrt{\frac{3}{q_1 q_2}}, \tag{4.22}$$

where $g(x)$ is a given function; therefore, these two conditions give the following expressions for the two constants C_1 and C_2 :

$$C_1(x) = \sqrt{8q_2}\left(\tanh\left(\sqrt{\frac{q_1 q_2}{3}}g(x)\right) - k\sqrt{\frac{1}{12}\frac{q_1}{q_2}}x\right), \qquad C_2 = 0.$$

We note that $C_1(x,t)$ is a quantity change with space and time, in which case the displacement takes the following form:

$$u(x,t) = \sqrt{\frac{3}{q_1 q_2}} \arctan\left(-k\sqrt{\frac{1}{12}\frac{q_1}{q_2}}t + \tanh\left(\sqrt{\frac{q_1 q_2}{3}}g(x)\right)\right). \tag{4.23}$$

Case (2).

If $\varkappa - \zeta < 0$, then both q_1 and q_2 are negative and $h > l_0$, l_1, and l_2, therefore, the expression for A (4.11) takes the following form, while the other quantities (q_1 and q_2) change their sign by choosing the the length–scale parameter related to the microinertia effect that is greater than the length–scale parameters related to the material in the sense of the modified strain gradient elasticity

$$A = -\frac{1}{12}\left|\frac{q_1}{q_2}\right|\frac{1}{(q_2)^2} < 0.$$

This Eq (4.10) takes the following form:

$$W'^2 = -A - 2|q_2|AW + \frac{1}{3}\frac{|q_1|}{|q_2|}W^2 + \frac{A}{1-2|q_2|W}, \tag{4.24}$$

where the same stipulation $-1/2q_2 < W < 1/2q_2$ is satisfied , allowing us to apply the binomial theorem for the last term in Eq (4.24) as follows:

$$\frac{A}{1-2|q_2|W} = A + 2A|q_2|W + 4A|q_2|^2W^2 + 8A|q_2|^3W^3 + 16A|q_2|^4W^4. \tag{4.25}$$

Substituting from Eq (4.25) into Eq (2.68), we have the following relation after some mathematical calculation and integration:

$$\int \frac{dW}{W^{3/2}\sqrt{1+2|q_2|W}} = i\sqrt{\frac{2}{3}|q_1|}\xi + C_1^*, \tag{4.26}$$

where C_1^* is the integration constant, and $i = \sqrt{-1}$.

Finally, obtaining the function U by performing the integration in Eq (4.26) and using $W = dU/d\xi$

$$U(\xi) = \int \frac{4}{-8|q_2| + \left(i\sqrt{\frac{2}{3}|q_1|}\xi + C_1^*\right)^2}d\xi + C_2^*, \tag{4.27}$$

where C_2^* is the integration constant.

Performing the integration in Eq (4.27) gives

$$U(\xi) = -\frac{\sqrt{3}}{i\sqrt{|q_1||q_2|}}\operatorname{arctanh}\left(\frac{\sqrt{\frac{2}{3}|q_1|}\xi + C_1^*}{\sqrt{8|q_2|}}\right) + C_2^*. \tag{4.28}$$

Consequently, the displacement field takes the following form:

$$u(x,t) = i\sqrt{\frac{3}{|q_1||q_2|}}\operatorname{arctanh}\left(i\sqrt{\frac{1}{12}\cdot\frac{|q_1|}{|q_2|}}k(x-t) + \frac{C_1^*}{\sqrt{8|q_2|}}\right) + C_2^*. \tag{4.29}$$

Here, C_1^* and C_2^* are integration constants determined from the initial and boundary conditions. These conditions are chosen in a suitable way to give three types of wave propagation as follows:

(a) Constant initial and boundary conditions
The following initial and boundary conditions are used to determine the constants C_1^* and C_2^* for the displacement field Eq (4.29):

$$u(0,0) = u_0, \qquad u(x \to \pm\infty, t) = \mp\frac{\pi}{2}\sqrt{\frac{3}{|q_1||q_2|}}. \tag{4.30}$$

Therefore, these two conditions give the following expressions for the two constants C_1^* and C_2^* :

$$C_1^* = \sqrt{8|q_2|}\tanh\left(-i\sqrt{\frac{|q_1||q_2|}{3}}u_0\right), \qquad C_2^* = 0,$$

then

$$u(x,t) = -\sqrt{\frac{3}{|q_1||q_2|}}\arctan\left(k\sqrt{\frac{1}{12}\frac{|q_1|}{|q_2|}}(x-t) - \tan\left(\sqrt{\frac{|q_1||q_2|}{3}}u_0\right)\right). \tag{4.31}$$

(b) Dynamical boundary condition
The boundary conditions are in the following form:

$$u(0,t) = f^*(t), \qquad u(x \to \pm\infty, t) = \mp\frac{\pi}{2}\sqrt{\frac{3}{q_1 q_2}}. \tag{4.32}$$

Therefore, these two conditions give the following expressions for the two constants C_1^* and C_2^*:

$$C_1^*(x,t) = \sqrt{8|q_2|}\left(\tanh\left(-i\sqrt{\frac{|q_1||q_2|}{3}}f^*(t)\right) + ik\sqrt{\frac{1}{12}\frac{|q_1|}{|q_2|}}t\right), \qquad C_2^* = 0,$$

then

$$u(x,t) = -\sqrt{\frac{3}{|q_1||q_2|}}\arctan\left(k\sqrt{\frac{1}{12}\frac{|q_1|}{|q_2|}}x - \tan\left(\sqrt{\frac{|q_1||q_2|}{3}}f^*(t)\right)\right). \tag{4.33}$$

(c) Static initial condition
The following initial conditions are used:

$$u(x,0) = g^*(x), \qquad u(x \to \pm\infty, t) = \mp\frac{\pi}{2}\sqrt{\frac{3}{|q_1||q_2|}}. \tag{4.34}$$

Therefore, these two conditions give the following expressions for C_1^* and C_2^* :

$$C_1^*(x) = \sqrt{8|q_2|}\left(\tanh\left(-i\sqrt{\frac{|q_1||q_2|}{3}}g^*(x)\right) - ik\sqrt{\frac{1}{12}\frac{|q_1|}{|q_2|}}x\right), \qquad C_2^* = 0,$$

then

$$u(x,t) = \sqrt{\frac{3}{|q_1||q_2|}}\arctan\left(k\sqrt{\frac{1}{12}\frac{|q_1|}{|q_2|}}t + \tan\left(\sqrt{\frac{|q_1||q_2|}{3}}g^*(x)\right)\right). \tag{4.35}$$

5. Numerical simulation

Let us choose the following data for the numerical simulation where $\rho = 2320\ \text{kg/m}^3$, representing the density; $\lambda = 5.44 \times 10^{10}\ \text{N/m}^2$ is Lame's constant; $\mu = 6.93 \times 10^{10}\ \text{N/m}^2$ is the shear modulus; h represents the internal length–scale parameter corresponding to the micro–inertia effect, and l_0, l_1 and l_2 are three material length–scale parameters related to the mathematical model and measured in nano–meters. The wavenumber and angular frequency are chosen in the form $k = 2\pi$ and $\omega = 1$; this choice leads to the vanishing of the quantity q_0. We study two cases below.

5.1. Case 1

In this case, we choose $h < l_0, l_1$ then $q_0 = 0$, $q_1 > 0$ and $q_2 > 0$, therefore, $\varkappa - \zeta > 0$, $h = 20 \times 10^{-9}$, and $l_0 = l_1 = 30 \times 10^{-9}$. The boundary conditions are described below.

(1) Constant initial and boundary conditions

In this case, we choose the initial condition $u(0, 0) = 1$. Then Eq (4.19) is considered along with the initial and boundary conditions given in Eq (4.18). Therefore, the figures illustrate the displacement field, the σ–stress tensor, the π–stress tensor, and the τ–stress tensor.

Figures 1–4 present a graphical simulation in a three-dimensional framework for kink, soliton, and bright–dark waves, respectively, corresponding to constant initial and boundary conditions (Eq (4.18)), applied at the lateral surface of the medium, within the framework of the MSGE theory. The kink wave is bounded, and the soliton wave propagates with constant amplitude and constant velocity. Two similar waveforms with different amplitudes, $\pi(x, t)$ and $\tau(x, t)$, are observed, corresponding, respectively, to the dilatation gradient vector γ_i and the deviatoric stretch gradient tensor $\eta^{(1)}_{i(jk)}$.

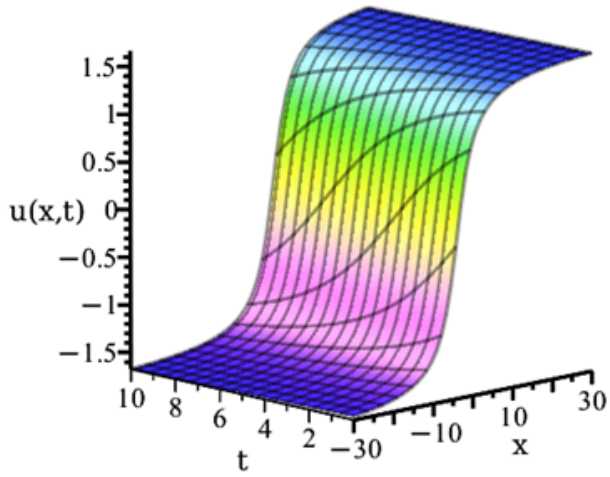

Figure 1. Displacement for $h < l_0, l_1$, and $\varkappa - \zeta > 0$.

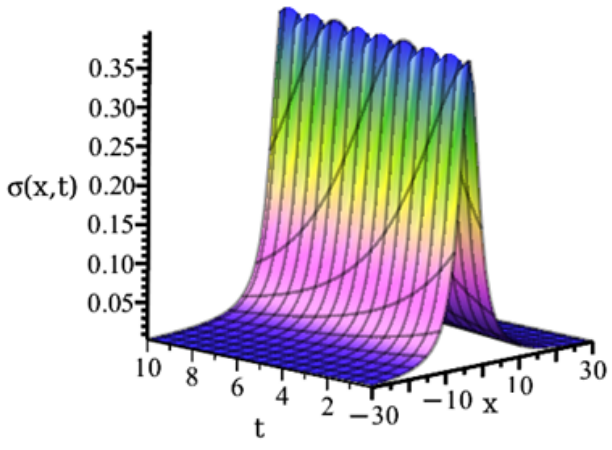

Figure 2. σ–stress for $h < l_0, l_1$, and $\varkappa - \zeta > 0$.

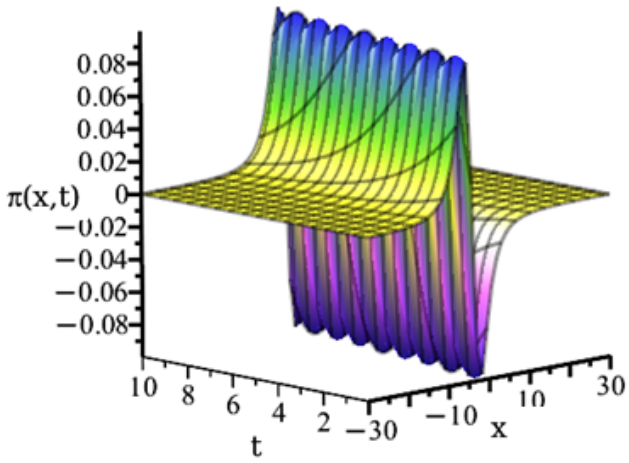

Figure 3. π–stress for $h < l_0, l_1$, and $\varkappa - \zeta > 0$.

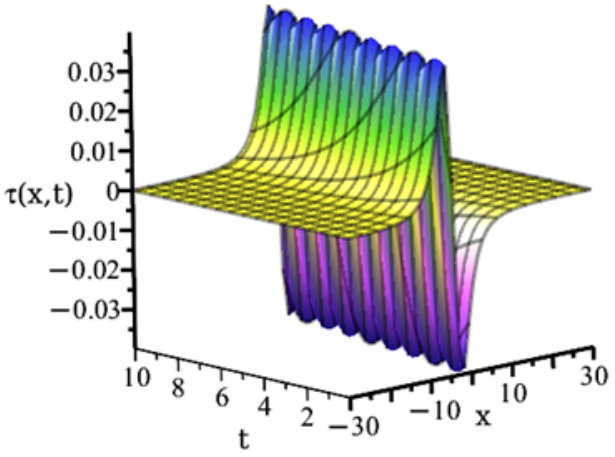

Figure 4. τ–stress for $h < l_0, l_1$, and $\varkappa - \zeta > 0$.

Figure 5 presents the propagation of a kink wave as a function of x at three different times. It is noted that the initial condition at the origin $(0, 0)$ is satisfied, and the wave remains bounded, i.e., $-\frac{\pi}{2}\sqrt{\frac{3}{q_1 q_2}} < u(x,t) < \frac{\pi}{2}\sqrt{\frac{3}{q_1 q_2}}$. Additionally, Figures 6–8 display the soliton and bright–dark waves as functions of x at three different time instances. It is observed that two waves, the π-wave and the τ–wave, propagate with different amplitudes through the elastic medium, with the $\tau(x,t)$–stress wave exhibiting greater damping than the $\pi(x,t)$-stress wave.

Moreover, both the soliton and dark–bright waves decay to zero as $x \to \pm\infty$, while propagating with constant velocities and amplitudes.

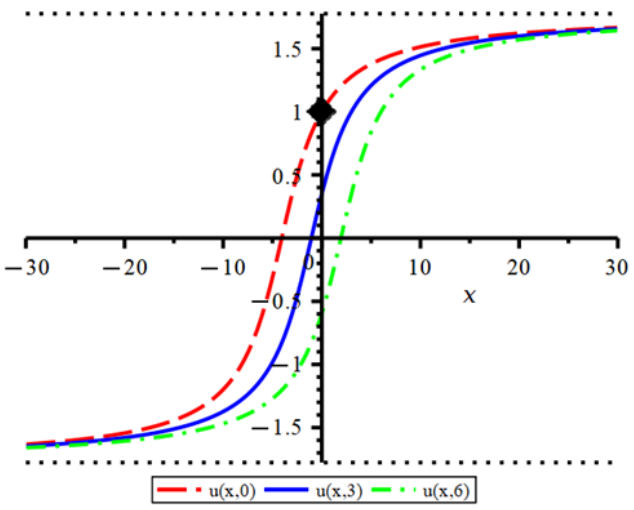

Figure 5. Displacement at $t = 0, 3$, and 6.

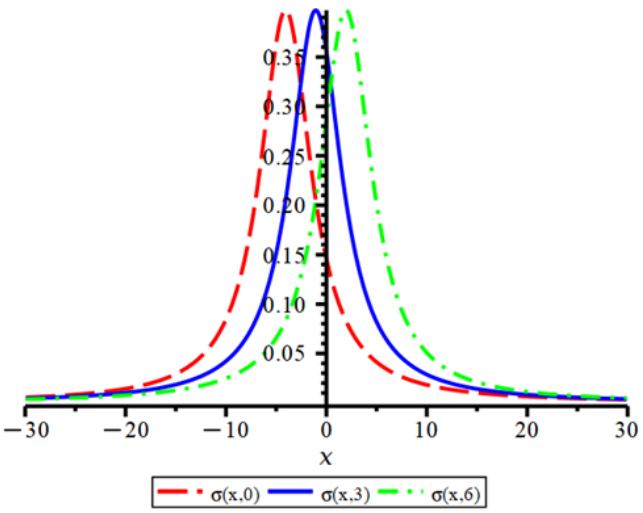

Figure 6. σ–stress at $t = 0, 3$, and 6.

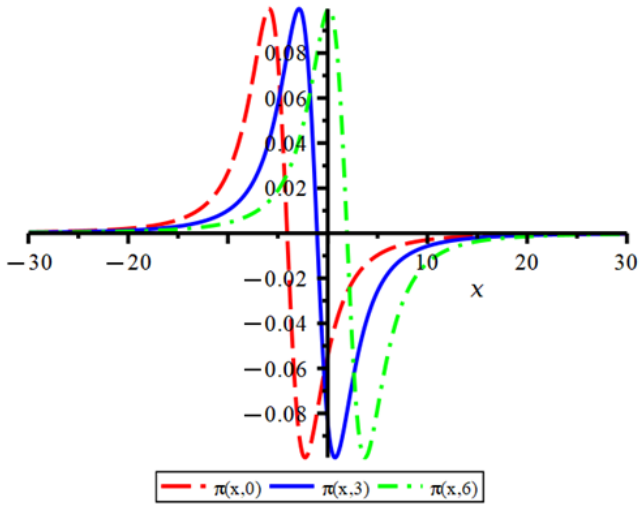

Figure 7. π–stress at $t = 0, 3$, and 6.

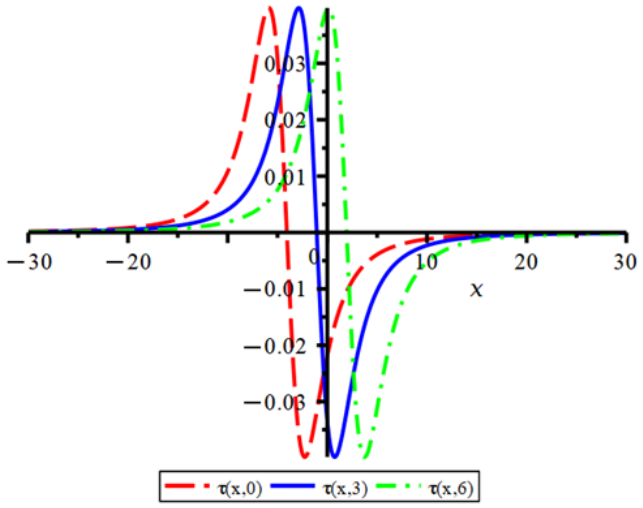

Figure 8. τ–stress at $t = 0, 3$, and 6.

(2) Dynamical boundary condition

In this part, we apply a dynamic boundary condition in the form

$$u(0, t) = -0.05 \exp(-0.8t)(1 - \cos(3t)),$$

which decays exponentially to zero with increasing time. Therefore, the corresponding three-dimensional representation is omitted due to its similarity to Figures 1–4. Instead, we present the following figures to illustrate the displacement field (Eq 4.21), the σ–stress tensor (Eq 3.10), the π–stress tensor (Eq 3.11), and the τ–stress tensor (Eq 3.12) at three different times with the initial and boundary conditions in (Eq 4.20).

It is noted from Figure 9 that the displacement wave resembles the shape of the incident wave and decays exponentially over time. Moreover, an observer located at $x = -0.05$ detects a wave with negative amplitude, while an observer at $x = 0.05$ detects a wave with a positive amplitude. In contrast, an observer at the origin detects no wave, indicating that the boundary condition is satisfied. Figures 10–12 represent the σ–stress, π–stress, and τ–stress, respectively. It is observed that all the waves decay exponentially over time, but with different amplitudes. Additionally, the $\pi(x, t)$ and $\tau(x, t)$ waves are similar in shape, both exhibiting negative amplitudes; however, $\tau(x, t)$–wave is more strongly damped than the $\pi(x, t)$–wave.

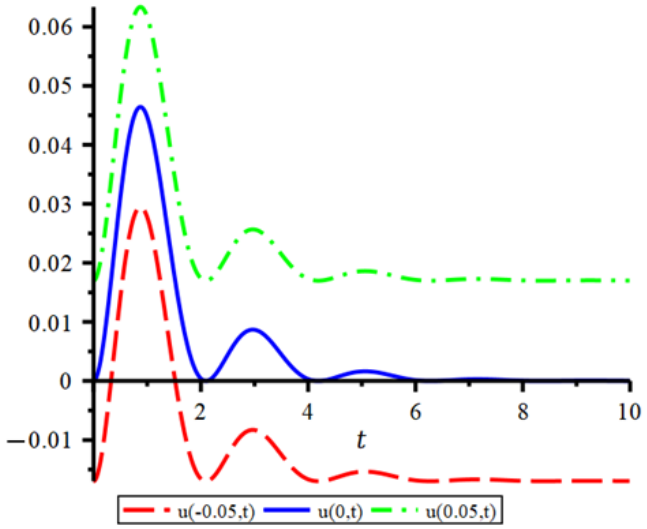

Figure 9. Displacement at $t = 0, 3$, and 6.

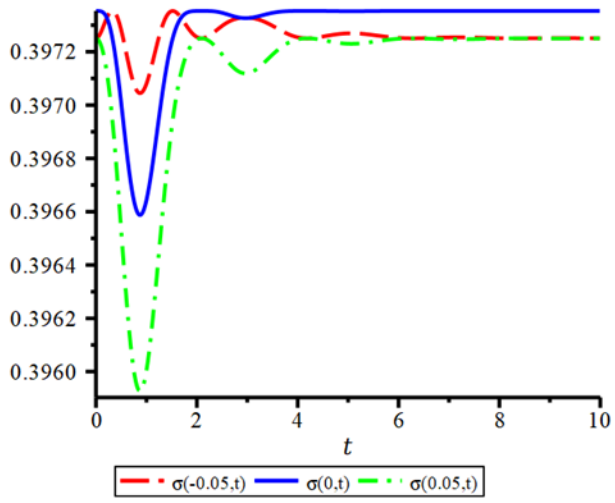

Figure 10. σ- stress at $t = 0, 3$, and 6.

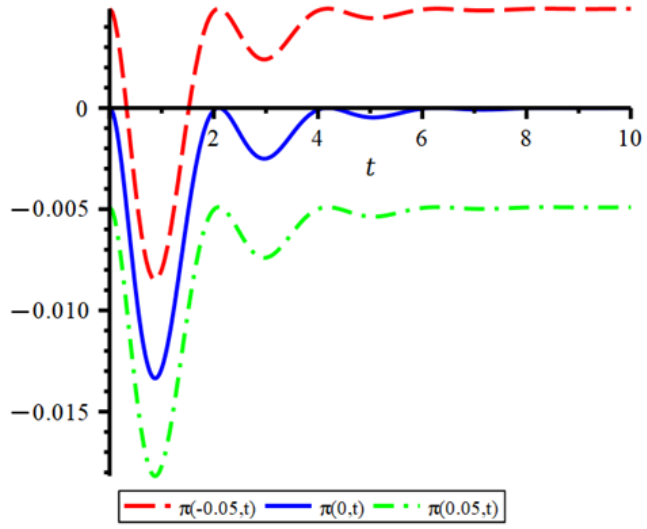

Figure 11. π- stress at $t = 0, 3$, and 6.

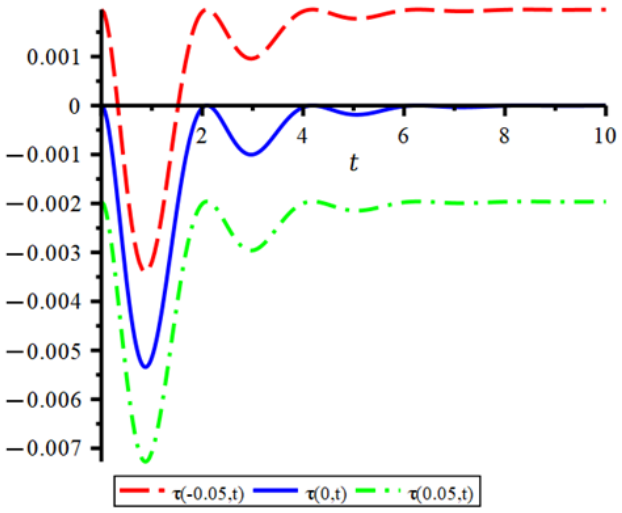

Figure 12. τ–stress at $t = 0, 3$, and 6.

(3) Static initial condition

In this section, we apply the static initial and boundary conditions given in equation (4.22), with the initial displacement defined as follows:

$$u(x, 0) = 0.5\text{sech}^2(-0.1x).$$

Accordingly, the following figures illustrate the resulting displacement field (Eq 4.23), the σ-stress tensor (Eq 3.10), the π-stress tensor (Eq 3.11), and the τ–stress tensor (Eq 3.12).

Figures 13–16 present three–dimensional numerical simulations for displacement, σ-stress, π–stress, and τ–stress, respectively. It is observed that the displacement wave represents a soliton with its maximum amplitude located at the origin. Figure 14 illustrates a bright–dark soliton wave.

Furthermore, Figures 15–16 depict dark–bright waves with negative amplitude, where the π-stress is more strongly damped than the τ–stress.

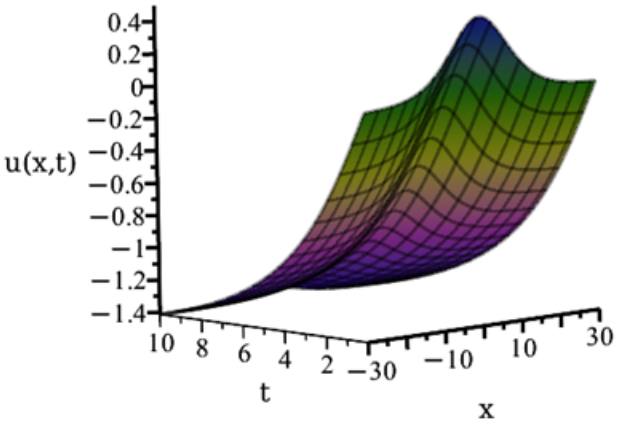

Figure 13. Displacement for $h < l_0, l_1$, and $\varkappa - \zeta > 0$.

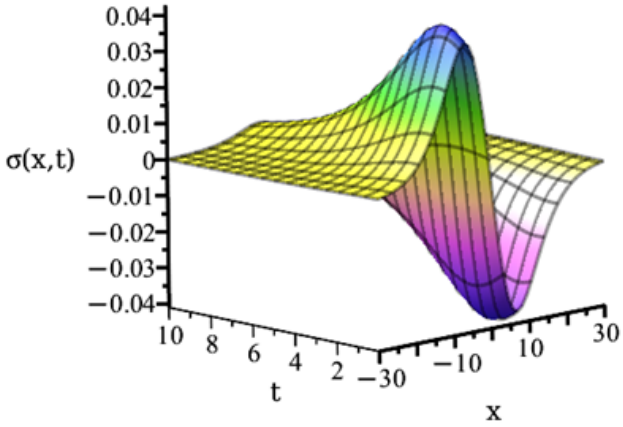

Figure 14. σ–stress for $h < l_0, l_1$, and $\varkappa - \zeta > 0$.

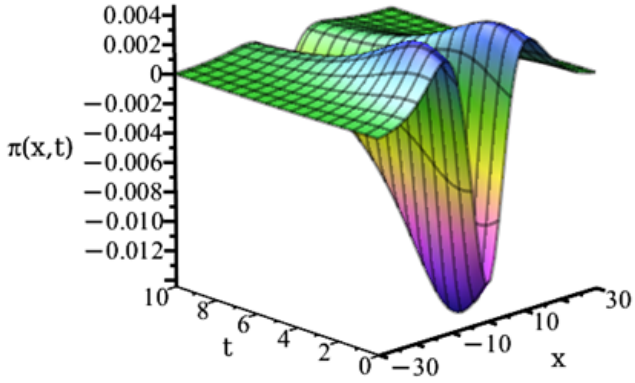

Figure 15. π–stress for $h < l_0, l_1$, and $\varkappa - \zeta > 0$.

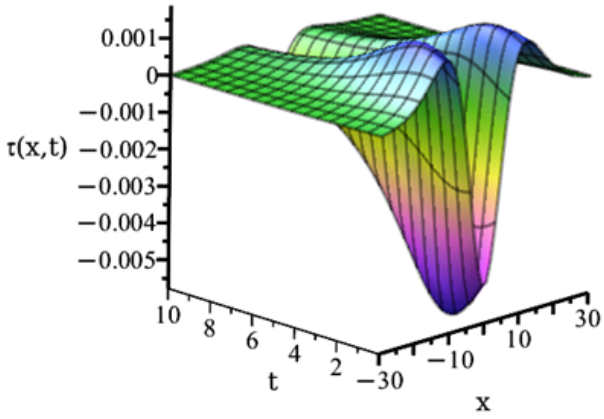

Figure 16. τ–stress for $h < l_0, l_1$, and $\varkappa - \zeta > 0$.

Figures 17–20 show the displacement, σ–stress, π–stress, and τ–stress at three different time values, respectively. It is noted that all observers along the x-axis detect the maximum amplitude of the displacement wave (Figure 17) at the origin. Moreover, the wave decays to zero at $t = 0$ as $x \to \pm\infty$, and decays to a constant value for the later time instances as $x \to \pm\infty$. In addition, the σ-stress decays to zero as $x \to \pm\infty$ and the wave attain its maximum amplitude within the interval $]-\infty, 0]$, and its minimum is within $[0, \infty[$, while damping over time. Figures 19–20 present the π–stress and τ–stress waves, which are similar in form, and both waves decay to zero as $x \to \pm\infty$. Moreover, the τ-stress is damped more than the π-stress.

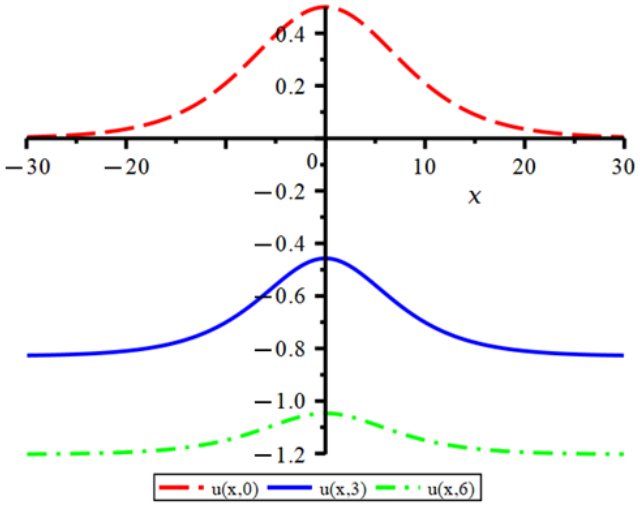

Figure 17. Displacement at $t = 0, 5$, and 10.

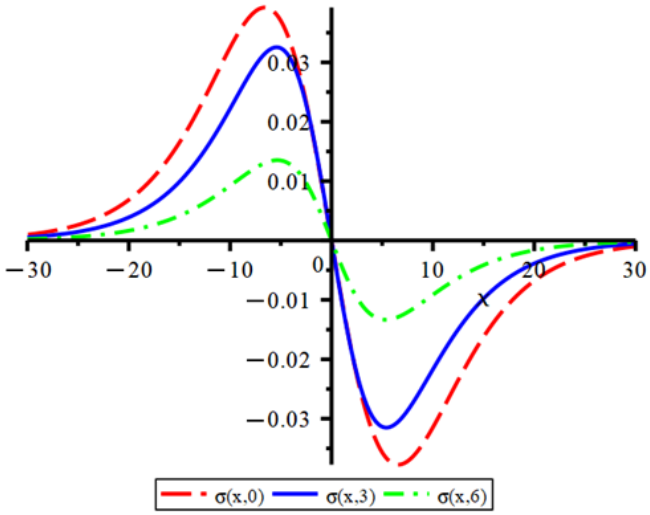

Figure 18. σ–stress at $t = 0, 5$, and 10.

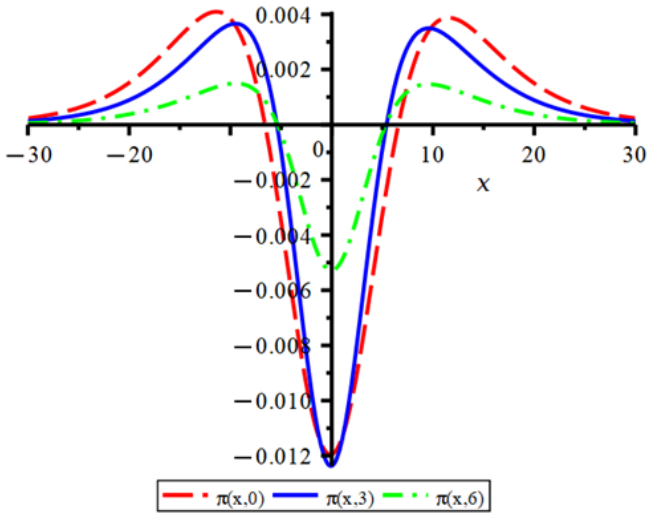

Figure 19. π–stress at $t = 0, 5$, and 10.

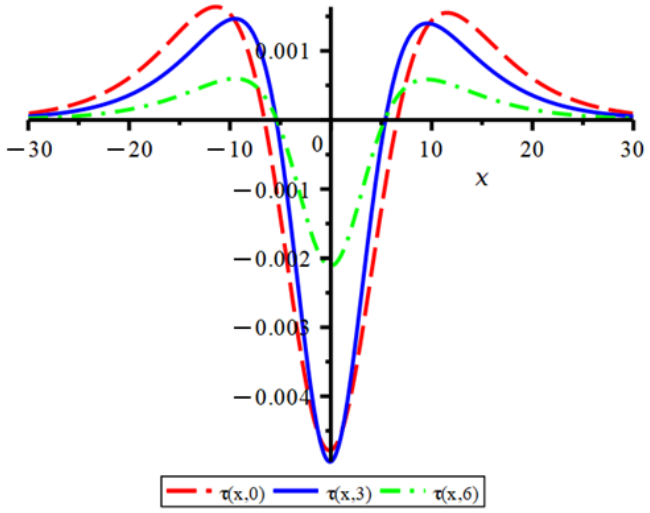

Figure 20. τ–stress at $t = 0, 5$, and 10.

5.2. Case 2

In this case, we choose $h > l_0$, and l_1 and thus $q_0 = 0$, $q_1 < 0$, and $q_2 < 0$; therefore, $\varkappa - \zeta < 0$, $h = 50 \times 10^{-9}$, and $l_0 = l_1 = 30 \times 10^{-9}$.

(1) Constant initial and boundary conditions

When we choose $u(0, 0) = 1$, according to Eq (4.29), the following figures (Figures 21–26) represent the displacement field, σ–stress tensor, π–stress tensor and τ–stress tensor.

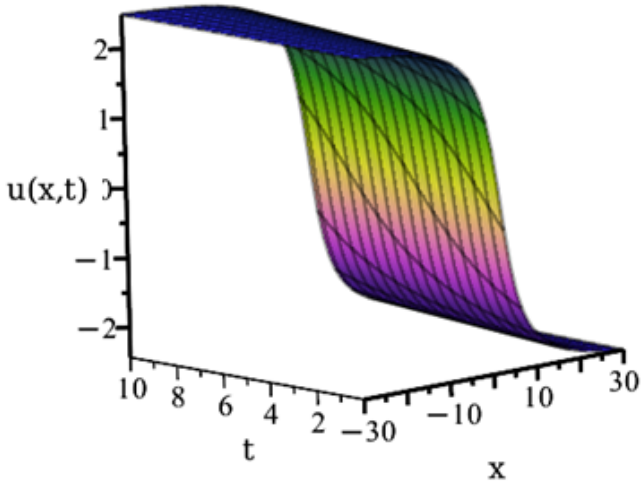

Figure 21. Displacement for $h > l_0, l_1$ and $\varkappa - \zeta < 0$.

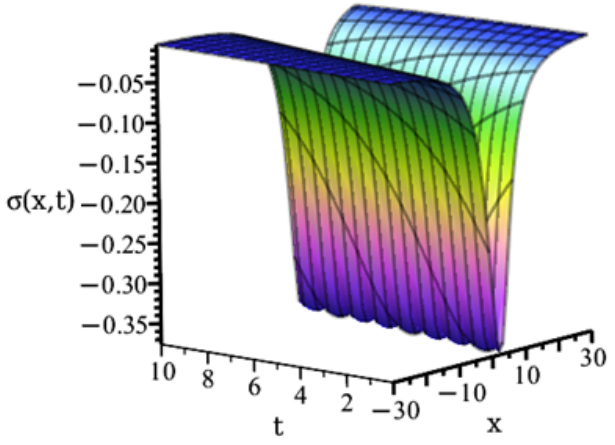

Figure 22. σ–stress for $h > l_0, l_1$ and $\varkappa - \zeta < 0$.

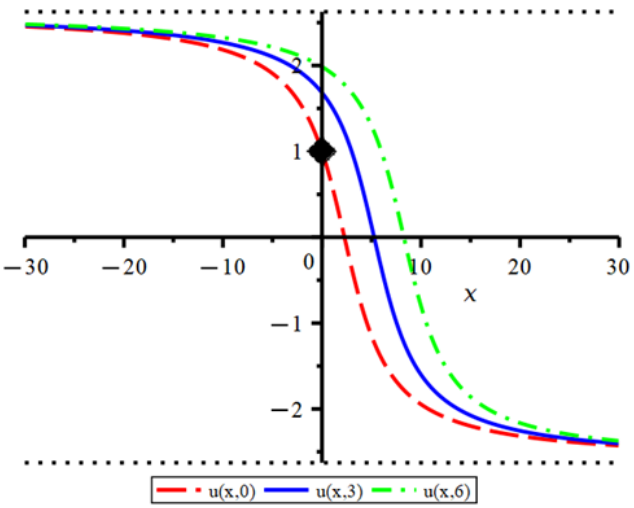

Figure 23. Displacement at $t = 0, 5, 10$.

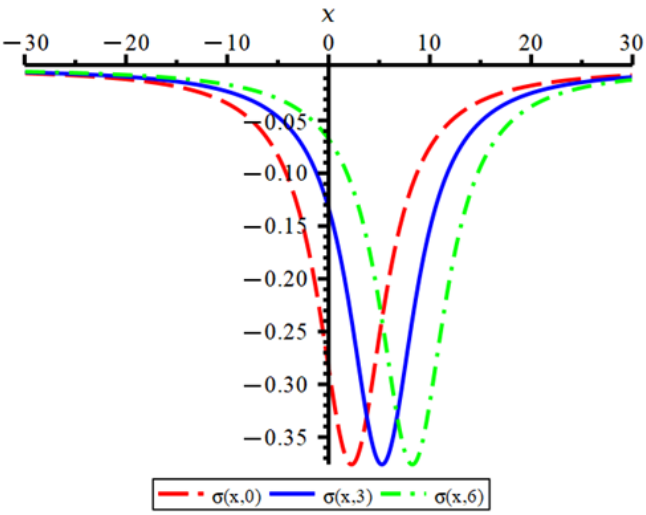

Figure 24. σ–stress at $t = 0, 2$, and 6.

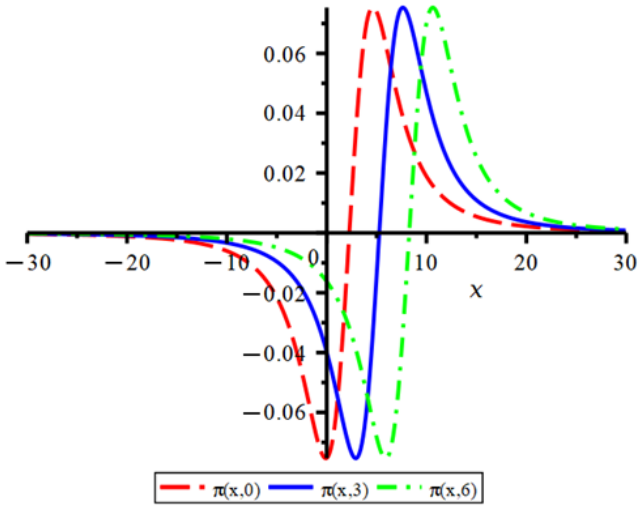

Figure 25. π–stress at $t = 0, 2$, and 6.

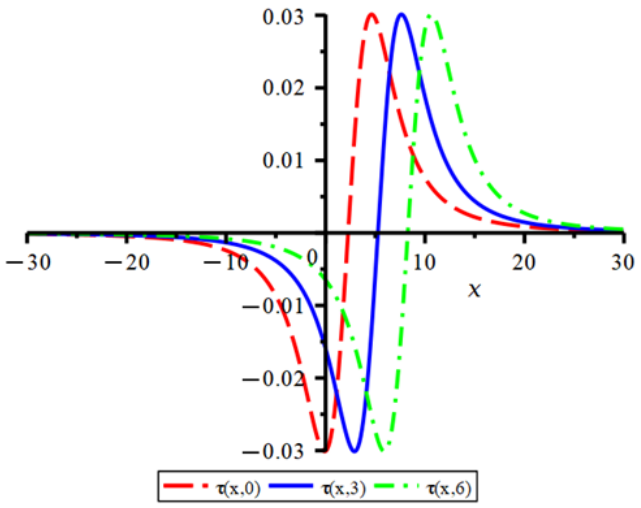

Figure 26. τ–stress at $t = 0, 2$, and 6.

Figures 21 and 22 present three–dimensional numerical simulations of an anti–kink wave and anti–soliton wave with a negative amplitude. Figures 23–26 illustrate additional simulation at three different instances, including anti–kink waves, anti–soliton, and dark–bright waves induced in the structures of the material. It is observed that the σ–stress, π–stress, and τ–stress waves decay to zero as $x \to \pm\infty$. Moreover, the τ–stress exhibits stronger damping compared with the π–stress.

(2) Dynamic boundary condition

In this part, we apply a dynamic boundary condition given by

$$u(0, t) = -0.05 \exp(-0.8t)(1 - \cos(3t)),$$

which decays exponentially to zero as time increases. As a result, we observe the formation of an anti-kink wave and an anti-soliton wave, similar to those shown in Figures 21 and 22. Additionally, the π–stress and τ–stress waves exhibit bright–dark soliton structures. These figures are omitted here for brevity. Moreover, the τ–stress wave is observed to be more strongly damped than the π–stress wave.

(3) Static initial condition

In this section, we apply the static initial condition

$$u(x, 0) = 0.5 \operatorname{sech}^2(-0.1x).$$

Accordingly, the displacement field given in Eq (4.35), together with the initial and boundary conditions specified in Eq (4.34), and the stress tensors σ, π, and τ, defined in Eqs (3.10)–(3.12), respectively, are illustrated in the following figures (Figures 27–30).

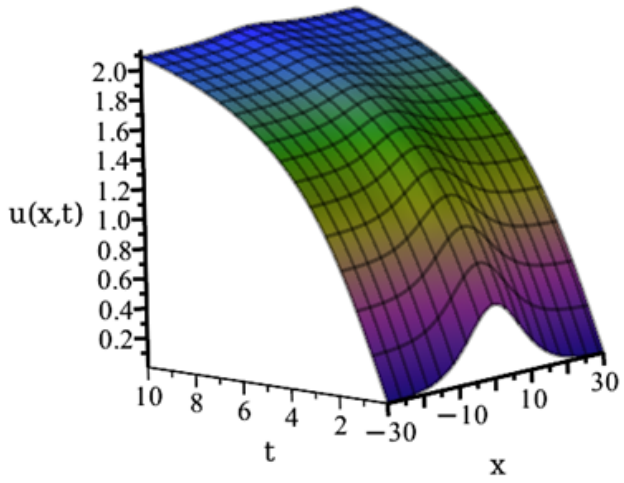

Figure 27. Displacement for $h > l_0, l_1$, and $\varkappa - \zeta < 0$.

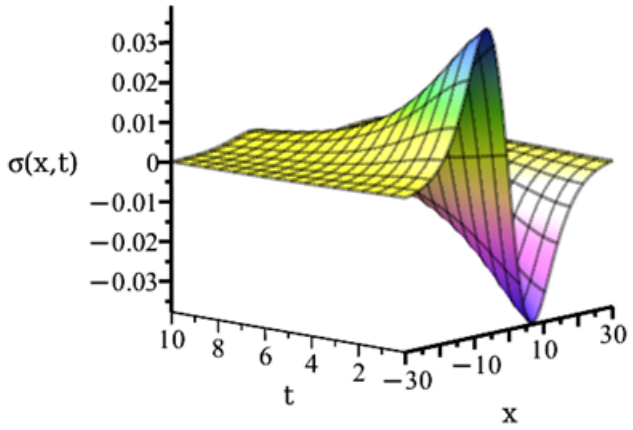

Figure 28. σ–stress for $h > l_0, l_1$, and $\varkappa - \zeta < 0$.

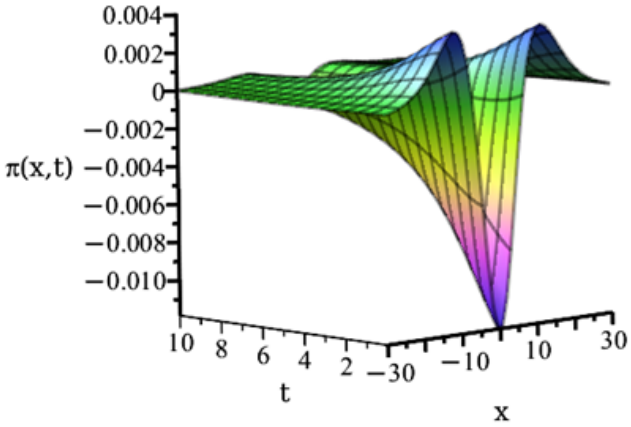

Figure 29. π–stress for $h > l_0, l_1$, and $\varkappa - \zeta < 0$.

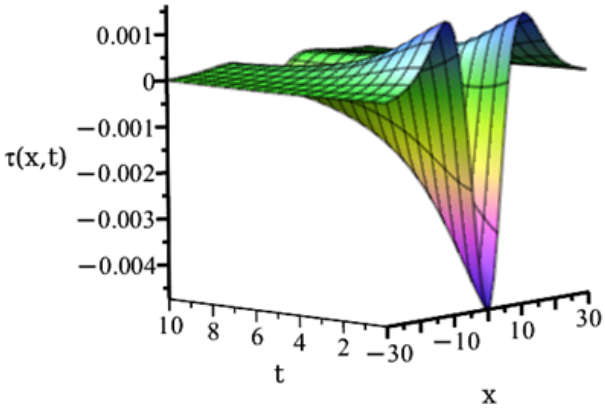

Figure 30. τ–stress for $h > l_0, l_1$, and $\varkappa - \zeta < 0$.

Here, Figures 27–30 represent three–dimensional graphical representation for soliton and bright–dark, and dark waves, respectively. It is observed that the σ–stress, π–stress, and τ–stress waves decay to zero as $x \to \pm\infty$. Moreover, the τ–stress exhibits stronger damping compared with the π–stress.

6. Conclusions

In this paper, we investigate the effects of nonlinear terms included in the MSGE theory by employing a variational principle. This approach is based on a strain energy functional and incorporates the virtual work done by external forces. Furthermore, we study the influence of the micro–inertia length–scale parameter, related to the internal structure of the elastic material, and the material length–scale parameters on wave propagation within the elastic medium. We analyze wave behavior at a unit of frequency under various initial and boundary conditions. Two cases are considered: $h > l_0$,

and l_1 and $h < l_0$, and l_1. In both cases, different wave propagation patterns emerge in the elastic material. Due to the nonlinear effects, kink and anti-kink waveforms are observed. Additionally, by appropriately tuning the material length–scale parameters, soliton and anti-soliton waves can also be generated. Another important observation obtained from the MSGE model is that the τ-stress wave, which is conjugate to the deviatoric stretch gradient tensor, is consistently more damped than the π-stress wave, which is conjugate to the dilatation gradient tensor in two cases. Finally, the results of this study indicate that by appropriately designing the internal structure of the elastic material, the type of wave induced within the medium can be effectively controlled.

The current study has several important potential applications, including the following:

- Designing engineering systems that block unwanted vibrations in mechanical or civil structures, thereby improving the stability and longevity of bridges, skyscrapers, and aircraft;
- Developing materials that guide, filter, or block sound and elastic waves at specific frequencies, which would be useful for soundproofing, acoustic cloaking, and noise control;
- Enhancing wave–based inspection techniques to improve sensitivity and resolution, enabling the detection of micro–defects or internal damage in materials with greater precision;
- Designing foundations or engineered soil layers that control or deflect seismic waves, offering passive protection against earthquakes for critical infrastructure;
- Embedding logic and wave-based computation into smart materials (mechanical computing), enabling them to respond adaptively to environmental stimuli;
- Tailoring wave propagation in tissue–mimicking materials to enhance the resolution and targeting capability of biomedical ultrasound imaging and therapies;
- Improving vibrational energy harvesting, allowing the conversion of wave energy into usable electrical power for small sensors and devices in remote or embedded applications.

Use of Generative-AI tools declaration

The author declares that they have not used Artificial Intelligence (AI) tools in the creation of this article.

Funding

This work was supported by the Deanship of Scientific Research, Vice Presidency for Graduate Studies and Scientific Research, King Faisal University, Saudi Arabia (Grant No–KFU253934).

Data availability

The datasets are available from the corresponding author on reasonable request.

Conflict of interest

The author declares that there is no conflict of interest regarding the publication of this paper.

References

1. A. R. Hadjesfandiari, G. F. Dargush, Couple stress theory for solids, *Int. J. Solids Struct.*, **48** (2011), 2496–2510. https://doi.org/10.1016/j.ijsolstr.2011.05.002
2. A. C. Eringen, Mechanics of micromorphic materials, In: H. Görtler, *Applied mechanics*, Springer, Berlin, Heidelberg, 1966, 131–138. https://doi.org/10.1007/978-3-662-29364-5_12
3. A. C. Eringen, Nonlocal continuum field theories, *Appl. Mech. Rev.*, **56** (2003), B20–B22. https://doi.org/10.1115/1.1553434
4. R. D. Mindlin, Micro-structure in linear elasticity, *Arch. Rational Mech. Anal.*, **16** (1964), 51–78. https://doi.org/10.1007/BF00248490
5. E. Cosserat, F. Cosserat, Théorie des corps déformables, *Nature*, **81** (1909), 67. https://doi.org/10.1038/081067a0
6. C. B. Kafadar, A. C. Eringen, Micropolar media–I the classical theory, *Int. J. Eng. Sci.*, **9** (1971), 271–305. https://doi.org/10.1016/0020-7225(71)90040-1
7. A. C. Eringen, Theory of micropolar continua, *Proc. Ninth Midwest. Mech. Conf.*, University of Wisconsin, New York: Wiley, 1965.
8. L. Dragos, Fundamental solutions in micropolar elasticity, *Int. J. Eng. Sci.*, **22** (1984), 265–275. https://doi.org/10.1016/0020-7225(84)90007-7
9. G. A. Maugin, Solitons in elastic solids (1938–2010), *Mech. Res. Commun.*, **38** (2011), 341–349. https://doi.org/10.1016/j.mechrescom.2011.04.009
10. V. Krylov, P. Rosenau, Solitary waves in an elastic string, *Phys. Lett. A*, **217** (1996), 31–42. https://doi.org/10.1016/0375-9601(96)00285-X
11. G. A. Maugin, A. Miled, Solitary waves in micropolar elastic crystals, *Int. J. Eng. Sci.*, **24** (1986), 1477–1499. https://doi.org/10.1016/0020-7225(86)90158-8
12. H. Demiray, S. Dost, Solitary waves in a thick walled elastic tube, *Appl. Math. Model.*, **22** (1998), 583–599. https://doi.org/10.1016/S0307-904X(98)10051-3
13. N. A. Fleck, G. M. Muller, M. F. Ashby, J. W. Hutchinson, Strain gradient plasticity: theory and experiment, *Acta Metall. Mater.*, **42** (1994), 475–487. https://doi.org/10.1016/0956-7151(94)90502-9
14. D. C. C. Lam, F. Yang, A. C. M. Chong, J. Wang, P. Tong, Experiments and theory in strain gradient elasticity, *J. Mech. Phys. Solids*, **51** (2003), 1477–1508. https://doi.org/10.1016/S0022-5096(03)00053-X
15. R. D. Mindlin, N. N. Eshel, On first strain-gradient theories in linear elasticity, *Int. J. Solids Struct.*, **4** (1968), 109–124. https://doi.org/10.1016/0020-7683(68)90036-X
16. B. S. Altan, E. C. Aifantis, On some aspects in the special theory of gradient elasticity, *J. Mech. Behav. Mater.*, **8** (2011), 231–282. https://doi.org/10.1515/jmbm.1997.8.3.231
17. D. Y. Yang, Z. Du, Asymptotic analysis of double-hump solitons for a coupled fourth-order nonlinear Schrödingier system in a birefringent optical fiber, *Chaos, Soliton. Fract.*, **199** (2025) 116831. https://doi.org/10.1016/j.chaos.2025.116831

18. Y. Zhang, D. Qiu, W. Liu, The Darboux transformation for the Tu equation: the kink and dromion solutions, *Eur. Phys. J. Plus*, **140** (2025), 657. https://doi.org/10.1140/epjp/s13360-025-06572-x.

19. P. Germain, The method of virtual power in continuum mechanics. Part 2: microstructure, *SIAM J. Appl. Math.*, **25** (1973), 556–575.

20. V. L. Berdichevsky, *Variational principles of continuum mechanics II: applications*, Springer, Dordrecht, 2009. https://doi.org/10.1007/978-3-540-88469-9 .

21. J. Kim, G. F. Dargush, Y. K. Ju, Extended framework of Hamilton's principle for continuum dynamics, *Int. J. Solids Struct.*, **50** (2013), 3418–3429. https://doi.org/10.1016/j.ijsolstr.2013.06.015

22. F. Dell'Isola, G. Sciarra, S. Vidoli, Generalized Hooke's law for isotropic second gradient materials, *Proc. R. Soc. A Math. Phys. Eng. Sci.*, **465** (2009), 2177–2196. https://doi.org/10.1098/rspa.2008.0530

23. L. Placidi, A. R. El-Dhaba, Semi-inverse method à la Saint-Venant for two-dimensional linear isotropic homogeneous second-gradient elasticity, *Math. Mech. Solids*, **22** (2017), 919–937. https://doi.org/10.1177/1081286515616043

24. A. R. El-Dhaba, Nonlinear deformation waves based on new Boussinesq-type equation within simplified strain gradient elasticity, *Math. Methods Appl. Sci.*, **48** (2025), 10841–10853. https://doi.org/10.1002/mma.10924

25. A. R. El-Dhaba, Periodic solutions for nonlinear deformation waves based on new Boussinesq-type equation within strain gradient elasticity and reductive perturbation technique, *Mech. Adv. Mater. Struct.*, 2024, 1–13. https://doi.org/10.1080/15376494.2024.2438905

AIMS Press